High-Throughput siRNA Screen Identifies MTX2 as a Novel Mediator of Mitochondrial Morphology

Matthew Gaetz

This thesis is submitted as partial fulfillment of the requirements for an M.Sc. in Cellular and Molecular Medicine from the University of Ottawa

August 2014

Department of Cellular and Molecular Medicine

Faculty of Medicine

University of Ottawa

© Matthew Gaetz, Ottawa, Canada, 2014

Abstract

Mitochondria exist in a dynamic network whereby fusion and fission events are critical to the health of the mitochondria, the cell, and the organism. Dysfunctional mitochondrial dynamics underlie a plethora of diseases including various cancers, heart diseases, diabetes, neurodegenerative diseases, and a number of mitochondrial disorders. Despite a strong molecular knowledge of a handful of functional mediators of mitochondrial dynamics, much less is known about how this process is regulated at a cellular level, and what genes are involved in signaling pathways. A previously completed mitochondrial morphology genome screen was repeated with an automated confocal microscope resulting in the identification and validation of MTX2 as a novel regulator of mitochondrial dynamics. Functional characterization of the role of MTX2 in mitochondrial dynamics will further our understanding of mitochondrial biology, and has the future potential to inform therapies for some of the many diseases underscored by dysfunctional mitochondrial dynamics.

Table of Contents

Figures

Abbreviations

AD	Alzheimer's disease
ADP	Adenosine diphosphate
AGO	Argonaute protein
ATP	Adenosine triphosphate
BAK	Bcl-2 homologous antagonist/killer
BAX	Bcl-2-associated X
BID	Bcl-2 interacting domain
BSA	Bovine serum albumin
C18ORF32	Chromosome 18, open reading frame 32
CCCP	Carbonyl cyanide *m*-chlorophenyl hydrazine
CHCHD3	Coiled-coil-helix-coiled -coil-helix domain containing 3
CMT2A	Charcot-Marie Tooth Type 2A
CJ	Cristae junction
DMSO	Dimethylsulfoxide
DNA	Deoxyribonucleic acid
DRP1	Dynamin-related protein 1
DTT	Dithiothreitol
ER	Endoplasmic Reticulum
ETC	Electron transport chain
FIS1	Mitochondrial fission protein 1
GFP	Green fluorescent protein
GHITM	Growth hormone inducible transmembrane protein
GSIS	Glucose-stimulated insulin secretion
GTP	Guanosine triphosphate
GTPase	Protein that hydrolyzes GTP
HD	Huntington's disease
HEK293T	Human embryonic kidney 293 cells with T-antigen
HeLa	Cervical cancer line derived from Henrietta Lacks

HIGD1a	Hypoxia-induced gene domain protein-1a
HTS	High-throughput screening
IMM	Inner mitochondrial membrane
IMS	Intermembrane space
LC3	Microtubule-associated protein 1A/1B-light chain 3
MAPL	Mitochondrial anchored protein ligase
MARCH5	Membrane-associated ring finger (C3HC4) 5
MEF	Mouse embryonic fibroblast
MiD49	Mitochondrial dynamics protein of 49kDa
MiD51	Mitochondrial dynamics protein of 51kDa
MIEF1	Mitochondrial elongation factor 1 (MiD51)
MIEF2	Mitochondrial elongation factor 2 (MiD49)
MFF	Mitochondrial fission factor
MFN1	Mitofusin 1
MFN2	Mitofusin 2
MitoPLD	Mitochondrial phospholipase D
MMACHC	Methylmalonic aciduria type C with homocystinuria
MMP ($\Delta\Psi$)	Mitochondrial membrane potential
MOMP	Mitochondrial outer membrane permeabilization
mtDNA	Mitochondrial DNA
MTX1	Metaxin 1
MTX2	Metaxin 2
MTX3	Metaxin 3
OMM	Outer mitochondrial membrane
OMA1	Overlapping with the m-AAA protease 1 homolog
OPA1	Optic Atrophy 1
OTE	Off-target effect
OXPHOS	Oxidative phosphorylation
PAGE	Polyacrylamide gel electrophoresis
PAH	Pulmonary arterial hypertension

PD	Parkinson’s disease
PINK1	PTEN-induced putative kinase 1
PKA	Protein kinase A
REDOX	Reduction/oxidation
RNA	Ribonucleic acid
RNAi	RNA interference
ROMO1	Reactive oxygen species modulator 1
ROS	Reactive oxygen species
SAM50	Sorting and assembly machinery component 50
SDS	Sodium dodecyl sulfate
SEC61β	Sec61 beta subunit
SENP5	Sentrin specific protease 5
siRNA	Small interfering RNA
SUMO	Small ubiquitin-like modifier
TNF	Tumor necrosis factor
TOMM20	20kDa translocase of the outer mitochondrial membrane
U2OS	Osteosarcoma cell line
UBC9	Ubiquitin carrier protein 9
VDAC1	Voltage-dependent anion channel 1
VEPH1	Ventrical zone expressing PH (pleckstrin homology) domain 1
WB	Western blot

Acknowledgements

Thanks first and foremost to my supervisor, Dr. Robert Screaton, for imparting guidance and wisdom over the last two years, as well as for funding my project from his existing grants. Thanks to Dr. Stephen Baird for his patience and knowledge relating to all things computer and image analysis. Thanks as well to all past and present members of the Screaton lab for their help and guidance, particularly MN, AN, and KR for training me. Thanks to all staff of CHEO, the CHEO RI, and particularly to Lynn Kelly for keeping everything running smoothly. Thanks to my TAC members and examiners, Dr. Martin Holcik and Dr. John Ngsee, Dr. Dave Stojdl and Dr. John Ngsee, respectively, for their time and expertise. Thanks to CIHR for funding this work.

Chapter 1. Introduction

1.1 Mitochondria and Mitochondrial Dynamics

Our understanding of mitochondria has changed dramatically since the coining of the term 'mitochondria' by Carl Benda in 1898[1]. Mitochondria originated from the phagocytosis of an α-protobacterium by the ancestral precursor of the eukaryotic cell approximately 2 billion years ago[2]. Over the course of evolution, the organelle gained a plethora of functions within our cells, while transferring most of its genome into the nucleus. A mitochondrion is comprised of about 1000-1500 proteins depending on the tissue, the vast majority of which are encoded by the nuclear genome, translated by cytosolic ribosomes, and translocated into mitochondria by various transporters[3, 4]. Mitochondria, themselves, retain about 16kb of circular DNA that encodes 13 genes comprising subunits of the mitochondrial respiratory complexes[3]. The mitochondrial genome also encodes 22 mitochondrial-specific transfer RNAs and 2 ribosomal RNAs[3].

The physical form of a mitochondrion is critical for its function[5]. Mitochondria exist as dual-membranous organelles, whereby an outer mitochondrial membrane (OMM) encapsulates a larger inner mitochondrial membrane (IMM) that is strategically folded to create invaginations known as cristae[6]. The compositions of the outer and inner membranes are highly ordered, with different sections containing distinct proteins and lipids, facilitating

functions such as protein transport or oxidative phosphorylation (OXPHOS)[7]. Mitochondria generate an electro-chemical proton gradient across their inner membrane (between the inter-membrane space (IMS) and the matrix), which is used to generate ATP. Reducing equivalents produced by the breakdown of fuel sources are passed along four electron transport chain (ETC) complexes (I, II, III, and IV) and in doing so, transfer protons from the matrix into the IMS. Protons then flow back through ATP synthase (complex V), which harnesses the potential energy of this electrochemical gradient to generate ATP. Cristae are the major site of ATP production owing to their compartmentalization of the ETC complexes and local restraint of metabolites [8, 9]. Different external and internal signals dictate the necessity and efficiency of OXPHOS, and the ETC complexes, as well as other integral mitochondrial membrane proteins, are dynamically assembled and rearranged in response to these signals[10, 11]. The electrochemical gradient generated by mitochondria also functions to facilitate protein and calcium import into the mitochondrion[3, 12], and loss of potential serves as a cellular signal of mitochondrial dysfunction[4].

As early as 1914, Lewis and Lewis described mitochondria as being motile organelles of changing shapes[13]. Many decades of research later, we have come to understand that mitochondria indeed exist in a dynamic network that is constantly engaged in fusion and fission events [*reviewed in 14*]. Collectively, mitochondrial fusion and division are known as mitochondrial dynamics. As the term 'mitochondrial dynamics' suggests, the morphology of a

cell's mitochondrial network is not static, but constantly changing. The opposing processes of mitochondrial fusion and fission exist in equilibrium in unstressed cells [15, 16]. Upon various stimuli, one process is increased and/or the other decreased resulting in either fragmentation or elongation of the mitochondrial network. Normal mitochondrial dynamics are required for apoptosis, development, proliferation, and mitochondrial quality control [*reviewed in 17*]. For this reason, dysfunctional mitochondrial dynamics underlie a massive number of diseases including: cancer, heart disease, Diabetes, Parkinson's disease, Alzheimer's disease, specific rare genetic disorders (Marie Charcot type 2A, Dominant Optic Atrophy), and numerous mitochondrial disorders. It is evident that mitochondrial dynamics is a fundamental cellular process, for which a greater understanding has the potential to lead to therapies for a wide variety of diseases.

1.2 Known Regulators of Mitochondrial Dynamics

1.2.1 Fusion Regulators

The Mitofusins 1 and 2 (MFN1 & MFN2) govern fusion of the outer mitochondrial membrane in vertebrates[18]. Both are large dynamin-like GTPase proteins that function by tethering the outer membranes of two mitochondria in close apposition[19]. It is formally unknown exactly how MFN1 and 2 catalyze membrane fusion, but it is likely resulting from their ability to self-assemble in *trans* and hydrolyze GTP, allowing lipid mixing between the two closely held membranes[17, 20]. Mitochondrial Phospholipase D (MitoPLD) is thought to

participate in this process by hydrolyzing cardiolipin to phosphatidic acid, which acts to either recruit fusion-mediating proteins, or directly as a fusogenic lipid itself[21-23]. Both MFN1 and 2 are ubiquitinated in response to loss of mitochondrial membrane potential, which leads to their proteasomal degradation[17, 24], however either Mitofusin can functionally compensate for loss of the other[25]. Loss of both mitofusins attenuates mitochondrial fusion, allowing the damaged mitochondrion to be segregated from the rest of the mitochondrial network and undergo mitochondrial autophagy (mitophagy)[24].

One main protein, Optic Atrophy 1 (OPA1), governs fusion of the inner mitochondrial membrane in vertebrates[26]. Like the mitofusins, OPA1 is a large GTPase that induces membrane fusion by tethering inner mitochondrial membranes into apposition[26]. The OPA1 gene is reported to contain as many as 8 splice variants[27]. OPA1 also contains two proteolytic cleavage sites, termed S1 and S2[28], which are cleaved by mitochondrial proteases YME1L[29, 30] and OMA1[31, 32], resulting in long and short isoforms[33]. Both long and short isoforms are required to support mitochondrial fusion [30-32]**.** Membrane-bound long Isoforms dimerize in *trans* to tether membranes together, allowing the soluble short isoforms to assemble into multimeric complexes where OPA1's GTPase activity mediates fusion of the two inner membranes[34]. Hypoxia-induced gene domain protein-1a (HIGD1a) has been shown to specifically bind OPA1 long isoforms, preventing their cleavage and promoting mitochondrial fusion[35].

In addition to its role in mitochondrial fusion, OPA1 plays a critical role in the assembly and maintenance of mitochondrial cristae by oligomerizing through its long and short isoforms to hold cristae junctions (CJs) together [36, 37]. The pro-apoptotic protein, truncated BID (tBid), permeates the OMM and disturbs OPA1 oligomers, resulting in CJ disassembly, cytochrome C release, and apoptosis[38]. Interestingly, OPA1's role in cristae integrity and apoptosis appears to be independent of its mitochondrial fusion function[38], and various groups have shown that cytochrome C release, triggering apoptosis, can be uncoupled from mitochondrial dynamics[39, 40].

Norton and colleagues have recently identified and characterized a novel IMM regulator of mitochondrial fusion, Reactive Oxygen Species Modulator 1 (ROMO1)[41]. ROMO1 is required for mitochondrial fusion, and without it cells exhibit a severely fragmented mitochondrial network. Loss of ROMO1 results in an accumulation of OPA1 isoform C, sensitization to apoptosis, and impaired mitochondrial respiration. Furthermore, ROMO1 can be oxidized to higher molecular weight species, which impairs mitochondrial fusion, whereas a non-oxidizable ROMO1 mutant promotes constitutive fusion[41]. This finding illustrates a previously un-described link between mitochondrial REDOX status and mitochondrial Dynamics[42].

1.2.2 Fission Regulators

Again, a single large dynamin-like GTPase, known as Dynamin Related Protein 1 (DRP1), is the main effector of mitochondrial fission in vertebrates.

Along with DRP1 are a host of accessory proteins that also contribute to fission, including: Mitochondrial Fission Factor (MFF), Mitochondrial Fission Protein 1 (FIS1), and the Mitochondrial Dynamics proteins of 49 and 51 kDa (MiD49 & 51; also known as mitochondrial elongation factor (MIEF) 2 & 1, respectively). DRP1 is a cytosolic protein that localizes to a mitochondrion, oligomerizes around it, and constricts in a GTP-dependent manner to cleave it [43-45]. It was long unknown both how DRP1 was signaled to cleave mitochondria at specific locations, as well as how DRP1 oligomers of ~100nm in diameter were able to divide a mitochondrion of ~500nm in diameter[46]. A landmark study by Friedman et al. partially answered both these questions by demonstrating that Endoplasmic Reticulum (ER) tubules mark sites of DRP1 recruitment and physically constrict the mitochondrion such that DRP1 oligomers can encircle it[47].

DRP1 is regulated by numerous post-transcriptional modifications, including: phosphorylation, ubiquitination, and sumoylation. Phosphorylation of DRP1 at S637 by protein kinase A (PKA) impairs its GTPase capability and results in mitochondrial network elongation[48, 49], whereas removal of a phosphate at S637 by the phosphatase calcineurin promotes DRP1 translocation to mitochondria and fragmentation[50]. Contrarily, phosphorylation of DRP1 at S616 by CDK1/Cyclin B promotes its fission activity, which is necessary for mitotic segregation of mitochondria[51]. DRP1 is ubiquitinated by the E3 ubiquitin ligases Parkin and MARCH5. While DRP1 ubiquitination by Parkin leads to its

proteasomal degradation[52], the effect of DRP1 ubiquitination by MARCH5 is much less evident. MARCH5 is an integral OMM protein that complexes with and ubiquitinates DRP1[53]. While both KD and overexpression of MARCH5 result in mitochondrial elongation, it is likely that this gene is involved in promoting fission by stabilizing DRP1 on the OMM[54-56]. The pro-apoptotic proteins BAK and BAX (which themselves have been reported to mediate mitochondrial fusion through activation of MFN2 [57]) are reported to promote DRP1 stabilization via sumoylation[58] through SUMO1[59], UBC9[60], and MAPL[61], whereas the protease SenP5 mediates DRP1 de-sumoylation[62, 63].

MFF is an OMM membrane protein that is believed to act as a receptor for DRP1, substantiated by the observations that KD of MFF leads to mitochondrial network elongation and reduced DRP1 recruitment[46, 64, 65]. The evidence supporting the role of FIS1 in mitochondrial dynamics are much more incongruous, and arise mostly through studies of the yeast DRP1 orthologue, DNM1. FIS1 is required as a receptor for DNM1 in yeast through its adaptor proteins MDV1 and CAF4 [66, 67]; and its overexpression leads to fragmentation, whereas it's inhibition leads to mitochondrial elongation[68]. There are no known MDV1 or CAF4 orthologues in mammals though[46], and FIS1 KO in HCT116 cells had no apparent effect on mitochondrial morphology[65]. More recently, Loson et al. performed immunofluorescence studies in MEFs re-affirming a role for FIS1 as a receptor for DRP1, and a component of mammalian mitochondrial fission machinery[46].

Even more complicated is the role of the MiD49 & 51 proteins in mitochondrial dynamics. Palmer et al. show that co-KD of the MiD proteins causes mitochondrial network elongation, however, both Palmer et al. and Zhao et al. show that overexpression of these proteins also causes mitochondrial network elongation [69, 70]. As studies by Loson et al. and Palmer et al. have demonstrated that the MiD proteins can mediate mitochondrial fission even in the absence of Mff and FIS1[46, 71], it is most likely that these proteins are mediators of mitochondrial fission. That their overexpression also results in mitochondrial network elongation can be explained as a dominant negative artifact, whereby under non-physiological conditions, the excess MiD proteins actually sequester DRP1 and prevent it from cleaving mitochondria[69, 71].

1.3 Normal Functions of Mitochondrial Dynamics

1.3.1 Apoptosis

Perhaps the most well characterized cellular process affected by mitochondrial dynamics is apoptosis. Apoptosis is the programmed death of cells, and is essential during normal eukaryotic development[72]. Furthermore, aberrant apoptosis underlies tumorigenesis (too little apoptosis)[73], as well as degenerative disorders (too much apoptosis)[74]. Apoptotic stimuli can be intra- or extracellular, but both converge on a signaling cascade that activates proteases, known as caspases[75, 76]. Caspases are activated through their own proteolytic cleavage cascade which serves to regulate their activity as well as amplify the apoptotic program[75]. In vertebrates, cytochrome C is the primary

internal stimulus of caspase activation, and as cytochrome C is normally sequestered in cristae of the mitochondrial matrix, mitochondrial control of cytochrome C release is a critical 'point of no return' in apoptosis[77].

The mediator of IMM fusion, OPA1, forms multimeric complexes of long and short isoforms, which tether CJs together and sequester Cytochrome C within the cristae[38]. The pro-apoptotic protein, truncated BID (tBid), disrupts OPA1 oligomers, allowing cytochrome C release from the cristae to the cytosol via mitochondrial outer membrane permeabilization (MOMP) induced by other pro-apoptotic proteins BAK and BAX[38, 78].

Dramatic mitochondrial network fragmentation is an early hallmark of apoptosis[79, 80]. Inducing mitochondrial fragmentation by increasing fission or preventing fusion sensitizes cells to apoptosis[81-84], whereas preventing fission or promoting fusion delays apoptosis[81, 83]. Furthermore, mitochondrial hyper-fusion has been observed as a pro-survival response to DNA/RNA damage[85]. Despite the intimate interplay between mitochondrial dynamics and apoptosis, several groups have shown that the two can be uncoupled [39, 40, 86], suggesting that mitochondrial fragmentation likely facilitates apoptosis, rather than is essential for it to occur.

1.3.2 Development/Proliferation

In addition to its well-characterized role in cell death, mitochondrial dynamics play a key role in other cell fates as well. MFN1, MFN2, OPA1, and DRP1 knockout mice are all embryonic lethal [87-89], collectively illustrating the

importance of these major dynamics regulators in normal development. Additionally, a girl with a dominant-negative DRP1 mutation displayed hypotonia, microcephaly, and optic atrophy before dying 37 days after birth; all defects were attributed to a lack of mitochondrial fission capability[90]. DRP1-mediated mitochondrial fission was also recently described as an essential signaling mechanism during constriction of the ductus arteriousus immediately following birth[91]. Moreover, mitochondrial dynamics are required to mobilize mitochondria into focal cellular regions with high energy demand, such as the distal synapses of neurons[92].

Mitochondrial dynamics play an integral role in cell proliferation as well. Mitochondria hyper-fuse their networks to promote more efficient energy production before entry into S-phase[93], at which point differential DRP1 phosphorylation promotes mitochondrial division to allow for segregation of mitochondria[51]. Not surprisingly, proper mitotic separation of mitochondria between mother and daughter cell requires mitochondrial fission as well [51].

1.3.3 Mitochondrial Quality Control

Owing to the importance of mitochondria in cellular function, cells understandably invest significant resources into ensuring that their mitochondria are healthy and functioning normally. Mitochondrial dynamics play two crucial, but distinct roles in mitochondrial quality control. Fusion between mitochondria allows the mixing of contents, including proteins, lipids and mtDNA, which allows damaged mitochondria to compensate by obtaining functional constituents from a

healthy mitochondrion[94-96]. In particular, individual cells, and even individual mitochondria will contain genetically variable mtDNA, a phenomenon known as heteroplasmy[96, 97]. Cells lacking mitofusin or OPA1 activity display a myriad of mitochondrial dysfunctions due to their inability to fuse[98], exemplifying the importance of mitochondrial fusion in normal mitochondrial function.

Alternatively, mitochondrial fission is essential for the selective removal and degradation of unsalvageable mitochondria through mitophagy[99]. Mitochondrial dysfunction resulting in loss of mitochondrial membrane potential (MMP, $\Delta\Psi$) prevents protein import, which results in the accumulation and stabilization of PTEN-induced putative kinase 1 (PINK1) on mitochondria[100-102]. PINK1 recruits Parkin to the damaged mitochondrial, where Parkin ubiquinates numerous proteins and recruits microtubule-associated protein 1A/1B-light chain 3 (LC3) to target the mitochondrion to the autophagosome[103-107]. Both mitofusins are degraded in response to Parkin-mediated ubiquitination, preventing the damaged mitochondrion from re-fusing with the mitochondrial network[24]. Furthermore, MFN2 phosphorylation by PINK1 is thought to act as a mitophagic signal[108].

1.4 Mitochondrial Dynamics in Disease

1.4.1 Cancer

Excessive proliferation and resistance to apoptosis are both well-documented hallmarks of cancer[109], and mitochondrial dynamics play key roles in both these processes. Generally cancer cell lines exhibit excessive fission as a

means of increasing their ability to undergo mitosis[110]. Lung cancers exhibit increased fission due to a preferential shift favoring DRP1 S616 over S637 phosphorylation, as well as decreased MFN2 levels[111]. Inhibition of mitochondrial fission leads to regression of lung tumors in a xenotransplantation model [111], and increased DRP1 expression in lung cancers is associated with a worse prognosis and chemotherapy resistance[112]. There is a paradox however, in that excessive fission, while supporting proliferation, also sensitizes cells to apoptosis and decreases efficiency of energy production. Hagenbuchner and colleagues provide a solution to this dilemma by demonstrating that neuroblastomas exhibit excessive DRP1-mediated fission, which favors the cancer cell undergoing aerobic glycolysis rather than OXPHOS[113]. Aerobic glycolysis is faster than OXPHOS at producing energy, allows shunting of metabolites to biosynthesis pathways, and facilitates metastasis[114], all of which confer an advantage to the neuroblastoma. To counter the increased sensitivity to apoptosis as a result of mitochondrial fragmentation, anti-apoptotic proteins are also up-regulated[113].

1.4.2 Pulmonary Arterial Hypertension & Reperfusion Injury

Much like the role of mitochondrial dynamics in cancer, an increase in fission and decrease in fusion permit the excessive proliferation of smooth muscle cells of the pulmonary artery leading to the pathogenesis of Pulmonary arterial hypertension (PAH)[110]. Both a decrease in MFN2-mediated fusion[115], and increase in DRP1-mediated fission[116] have been reported in

pulmonary arterial hypertension, with an increase in fusion providing a beneficial therapeutic outcome[115]. Alternatively, decreased OPA1 levels resulting in an increase in apoptosis were observed in failed human hearts, removed following transplantations[117]. Separately, inhibition of DRP1 through a small molecule inhibitor, mdivi1, or with siRNA, has been shown to be an effective novel strategy for improving myocardial function in a mouse model of ischemic reperfusion injury [118].

1.4.3 Neurodegenerative Disorders

Unlike disorders of excessive proliferation (cancer, PAH) where excessive fission provides cells with a proliferative advantage, neurodegenerative disorders are usually characterized by excessive mitochondrial fission leading to a sensitization to apoptosis and unhealthy levels of mitophagy [110]. Mitochondrial dysfunction and impaired mitochondrial dynamics are a common link between all major neurodegenerative disorders and neuropathies, likely because neurons require large focal concentrations of energy and thus rely heavily on their mitochondria [119]. Parkinson's disease (PD) is both a sporadic and genetic disease, characterized by the loss of dopaminergic neurons as a result of mitochondrial dysfunction[120]. Mitochondrial dynamics are intimately linked to PD through their influence on mitochondrial quality controls pathways[121]; the two most common monogenic forms of PD arise from mutations of the Parkin and PINK1 genes[120]. Parkin, named for its role in familial Parkinson's disease (PD), normally ubiquitinates DRP1, leading to its proteasomal degradation[52].

Mutations affecting Parkin function result in abnormally high DRP1 levels, which results in excessive mitochondrial fission and contributes to neurodegeneration[52].

In Huntington's Disease (HD), CAG nucleotide repeats result in a mutated huntingtin protein containing a series of abnormal glutamine residues[122]. Song et al. show that mutant huntingtin binds DRP1, increasing its fission activity and sensitizing neurons to apoptosis, contributing to pathogenesis of the disease[123]. Amyloid-beta plaques, which are characteristic of Alzheimer's disease (AD) pathogenesis, have been shown to increase levels of FIS1 and alter mitochondrial morphology in an AD model[124]. Additionally, in hippocampus samples of AD patients, Wang et al. report reduced levels of MFN1 & 2, OPA1, and DRP1, but increased levels of FIS1, collectively resulting in abnormal neuronal mitochondrial distribution, which could be reverted in an AD M17 cell model through overexpression of DRP1[125]. It is evident that mitochondrial dynamics are required to maintain proper mitochondrial function, and dysfunctional mitochondrial dynamics exacerbates the pathogenesis of major neurodegenerative disorders. Even further illustrating the role of mitochondrial dynamics in neuronal health is the finding that DRP1 inhibition protects primary neurons from acute ischemic brain injury[126].

1.4.4 Neuropathies

In addition to the widespread effects of dysfunctional mitochondrial dynamics on neurodegenerative diseases, there are a handful of neuropathies

resulting from specific mutations in known regulators of mitochondrial dynamics. Mutations in the coiled-coil or GTPase regions (both are required for fusion) of MFN2 result in Charcot-Marie type 2A syndrome, which is characterized by foot deformities, atrophy of lower legs, and abnormal gait[110, 127]. MFN2 mutations have also been found to cause peripheral neuropathy, cognitive impairment, and lipodystrophy[128, 129]. Likewise, mutations in the GTPase domain of OPA1 result in optic atrophy, which is characterized by progressive blindness. Without OPA1 fusion activity, optic neurons die from unbalanced fission, resulting in sensitization to apoptosis[86].

1.4.5 Diabetes

As diabetes mellitus and obesity-induced insulin insensitivity are both diseases with strong metabolic and degeneration links, it is no surprise that mitochondrial dynamics play a role in the pathogenesis of these disorders. Patients with type II diabetes, or that are obese, display decreased MFN2 levels and decreased fusion activity[130]. Similarly, hepatic ablation of MFN2 resulted in impaired insulin signaling and glucose tolerance[131]. β-cell-specific OPA1 KO mice display impaired glucose stimulated insulin secretion (GSIS) and develop hyperglycemia[132], collectively illustrating the importance of mitochondrial dynamics in normal β-cell function.

1.5 High-Throughput Genome Screening

1.5.1 RNA Interference

RNA interference (RNAi) was first identified with the introduction of double-stranded RNA (dsRNA) into C. elegans, which resulted in loss of genes containing sequences complementary to the introduced dsRNA[133]. Since its discovery, RNAi pathways have been found to exist is most eukaryotes, including humans, and are thought to have emerged as an innate defense against viral infection [134, 135], and later found to be able to regulate gene expression[136, 137]. In animals, RNAi is mediated through small-interfering RNAs (siRNAs) and micro RNAs (miRNAs), both of which are short double stranded RNA sequences of ~21 nucleotides[134, 136, 138]. A conserved RNase III ribonuclease family member, termed Dicer, was found to be the enzyme responsible for cleaving dsRNA or short-hairpin RNA (shRNA) into specific siRNA/miRNA oligonucleotides[134, 136]. Following cleavage by Dicer, siRNA/miRNA oligonucleotides are loaded into the RNA-induced silencing complex (RISC), which, with the help of Argonaute (AGO; AGO2 in humans[139]) proteins, unwinds the siRNA and cleaves the passenger strand, while retaining the guide strand [136, 139-141]. The RISC complex then binds via its guide strand to target (complementary) mRNA in order to sequester and degrade it[140, 142, 143]. Knowledge of these pathways has transformed them into powerful cell biology tools, whereby synthesized siRNA duplexes can be transfected into cells, resulting in transient loss of a target gene's protein levels known as knockdown

(KD). Alternatively, shRNAs can be packaged into lentivirus and incorporated into an infected host cell's genome, providing stable knockdown of the target gene.

1.5.2 Genome Screens

Functional elucidation of an unknown gene *in vivo* has been traditionally performed through loss-of-function experiments, which are extremely resource and labor-intensive[144]. The discovery and application of RNAi, combined with sequencing of the human genome, has made it possible to perform loss-of-function experiments in high-throughput. Likewise, advances in biotechnology and computing power permit the generation and analysis of massive data sets. The idea of screening is to identify novel targets, either small molecule or gene, that affect a biological system of interest. Screens can be carried out to find multiple novel targets that affect a given biological system, or to find a single target, which was previously unknown but presumed to exist [145-148]. While large high-throughput screens are usually carried out in cell lines for reagent availability and reproducibility, some groups have performed RNAi screens in full organisms including C. Elegans and mice[147, 149].

Despite the powerful applications of high-content screening, they are not without disadvantages and caveats as well. Notably, in the case of RNAi screens, there is a significant concern of off-target effects (OTEs), leading to the "identification" of false positives[150, 151]. Off-target effects arise from a promiscuity of si/shRNA sequences, leading to the sequestration or degradation of unintended transcripts[152], as well as potential unrelated phenotypes simply

as a result of siRNA transfection[150]. Despite an ever-increasing molecular understanding of RNAi pathways, we remain incapable of predicting off-target effects based on siRNA sequence[152]. Furthermore, Khan et al. have suggested that siRNA introduction can affect endogenous miRNAs, altering global gene expression[153]. The prevalence of OTEs requires extensive validation of screen 'hits' be undertaken in order to establish them as true positives.

1.5.3 Candidate Selection and Validation

Following the completion of a screen, top candidates are selected for validation via a thorough analysis of the screen data. Methods for analyzing screen data will depend on the biological process being assayed, as well as the readout for that process. Due to the sheer size of genome screens, there will be inevitable variability between plates. Various methods of normalization can be used to account for this effect of random variation (reviewed in [154]), with no clear cut best method of normalization having emerged[155]. Generally, a robust Z-score is used in RNAi screens to rank the normalized data[154]. Robust Z-scores use the median and median absolute deviation (MAD) in place of the mean and standard deviation (used for z-scores), which makes them insensitive to the effects of outliers and preferable in the case of RNAi screens[156]. From the robust Z-scores, a list of top candidates can be selected.

Owing to the aforementioned OTEs of RNAi, a candidate gene must be validated as a 'true' effector of the biological process for which one is screening. The only unequivocal way to do this is through a 'rescue' experiment, whereby an

si/shRNA-resistant cDNA is introduced into cells lacking that gene, leading to reversion of the phenotype generated by knockdown of that gene[144, 157]. Rescue experiments, however, are time and resource expensive, as well as fraught with their own caveats, so before devoting significant time to rescuing a gene, a secondary validation (secondary screen) of the candidates is recommended. Secondary screens can be performed with deconvoluted siRNAs or shRNAs, with the goal of observing multiple independent RNAi reagents eliciting the same phenotype[144].

1.6 Summary

It is evident that mitochondrial dynamics are intimately involved in both mitochondrial quality control and apoptosis, making them critical for cellular and whole organism health. A myriad of diseases are implicated with dysfunctional mitochondrial dynamics, further illustrating the importance of this cellular process. Several large dynamin-like proteins have been identified and extensively characterized as effectors of mitochondrial dynamics. The signaling pathways, and accessory proteins that govern mitochondrial dynamics are much less well known. My Masters thesis project sought to use high-throughput siRNA screening to identify novel regulators of mitochondrial dynamics.

Chapter 2. Materials and Methods

2.1 Antibodies

β-Actin (Sigma, 1:20000); C18ORF32 (Santa Cruz, 1:1000); Cytochrome C (BD Pharmingen, 1:1000); DRP1 (BD Bioscience, 1:1000); GHITM (Abnova, 1:1000); HSP90 (Santa Cruz, 1:1000); MFN1 (Abcam, 1:500); MFN2 (Abnova 1:1000); MTX2 (Santa Cruz, 1:1000); MMACHC (Abcam, 1:500); Opa1 (Abcam, 1:1000); Tomm20 (Santa Cruz, 1:2000); Ubiquitin (Cell Signaling, 1:1000); V5 (Invitrogen, 1:2000); VDAC1 (Cell Signaling, 1:1000); VEPH1 (Abcam, 1:1000); Secondary antibodies conjugated to fluorophores were all obtained from Invitrogen.

2.2 Reagents

Lipofectamine RNAiMAX, Hoechst 33342, TMRE, Phusion DNA polymerase, and BP & LR clonases were all from Invitrogen. CCCP, BSA, DMSO, Doxycycline, MG132, and all common chemicals were from Sigma. QVD was from Calbiochem. Adeno tBid was a gift from Gordon Shore, McGill University. All siRNAs were obtained from Dharmacon. Restriction enzymes were from NEB.

2.3 Cloning and Lentivirus Generation

RNA was harvested from cultured cells, and cDNA was generated through a reverse transcriptase reaction. Genes were amplified from cDNA using primers containing gateway 'ATTB' sites, and amplified products were recombined into a pDONR vector with BP clonase, then flipped into modified pLenti6 vectors with LR clonase. For shRNA, custom oligonucleotides encoding shRNA sequences

were purchased from Integrated DNA Technologies (http://www.idtdna.com/site), and ligated into modified pLKO.1 vectors. Lentivirus was generated through transfection of PCMV8.74, PMD2.G, and pLenti6/pLKO.1 plasmids into HEK293T cells. 72h following transfection, media was collected, and viral particles were concentrated and purified through a 20% sucrose gradient by ultracentrifugation (28,000rpm, 4°C, 2h).

2.4 Cell lines

HeLa and HEK293T cells were cultured in DMEM (Thermo Scientific) containing 5% FBS, and penicillin/streptomycin. U2OS cells were cultured in McCoy's 5A medium (Thermo Scientific) containing 5% FBS, penicillin/streptomycin and blastocidin/zeocin. U2OS Sec61β-mcherry cells were generated by Andy Ng.

2.5 Original Genome Screen & Quantification of Mitochondrial Morphology

The first genome screen was carried out as described previously by Norton et al[41]. All quantification of mitochondrial morphology was performed as previously described by Norton et al.[41]; 15 fields per well were visualized with the Cellomics Arrayscan automated microscope system.

2.6 Genome Screen Repeat

Pooled siRNAs were previously aliquoted into Aurora 384-well glass bottom plates (Brooks Life Sciences), and frozen at -20°C in a frost-free freezer. The screen was divided into quarters for technical reasons, and performed in triplicate (198 plates total). All reagents were made prior to the screen and were 0.22um

filter sterilized. HeLa cells (p14) were aliquoted from a common pool and frozen in liquid nitrogen. 1 week prior to the start of each quarter, 1 aliquot of HeLa cells was thawed and passaged twice. Using a robotic multidrop, HeLa cells (450/well; 15,000/mL) were reverse transfected with siRNA pre-incubated with Lipofectamine RNAiMAX (5uL/mL) in 2X OPTIMEM. 72h following transfection, cells were fixed in 3.7% formaldehyde and 1ug/mL Hoechst. After 1-2h of fixing at 37°C, fixative was removed and replaced with PBS containing 1% glycine. Glycine-PBS was aspirated and cells were washed once with PBS, then incubated 1-2h with a 0.1% Triton-X-100, 3% BSA in PBS solution (1-2h incubation at room temperature). Cells were then washed with PBS and incubated overnight (4°C) with 3% BSA in PBS containing 1:1000 Rabbit anti-Tomm20 antibody. The following day, cells were washed with PBS and incubated 1-2h with anti-rabbit 594 secondary antibody in 3% BSA-PBS. Cells were then washed 3 times with PBS, and plates were sealed and stored at 4°C for up to 2 weeks prior to imaging. For each well, Mitochondria and Nuclei in 42 fields were visualized using 40X objective of the OPERA automated confocal microscope system (Perkin Elmer). Imaging took approximately 2 weeks for each quarter (~50 plates) of the genome set. Images were then uploaded into the image analysis software Columbus (Perkin Elmer), which took approximately another 2 weeks per quarter. Algorithm development and validation was performed by Dr. Stephen Baird and is ongoing as of May 2014.

2.7 Confocal Microscopy

Cells were transfected/infected and immunostained as described above. Cellular components were visualized using the Olympus Fluoview FV1000 Confocal Laser Scanning Biological Microscope. Image analysis was performed using Fluoview software from Olympus.

2.8 Western Blotting

Cells were washed once with PBS, then lysed and protein was harvested in 1% SDS Lysis buffer containing 50mM DTT. Samples were separated by SDS PAGE and transferred onto a PVDF membrane (Millipore, Fisher). Western blotting was performed in 5% milk in TBS with 0.1% Tween 20 using the antibody concentrations described above. Membranes were exposed with ECL or ECL' Western blotting reagent from Amersham.

2.9 Cytochrome C Release Assay

72h following transfection (performed as described above) cells were treated with Adenovirus expressing doxycycline-inducible tBid, 12.5uM QVD, and 1ug/mL doxycycline, then incubated for 4h or 8h. Cells were fixed in 3.7% formaldehyde and Hoechst and immunostained for Tomm20 and cytochrome C, prior to being imaged by the Cellomics Arrayscan microscope. Images were analyzed using an algorithm that quantifies the colocalization between mitochondria (Tomm20) and cytochrome C.

2.10 Statistics

The median aspect ratio score of three technical replicates was normalized against the control siRNA on each plate of the original genome screen. Robust Z-scores were calculated as: (x – median(samples)) / (MAD)*1.4826). Two-tailed Student's T-test was used to assess the significance between biological conditions in non-screen experiments.

Chapter 3. Results

3.1 First Mitochondrial Morphology Screen

Preceding the beginning of my Masters Thesis Project, Andy Ng, Dr. Stephen Baird, and principal investigator, Dr. Robert Screaton, carried out a genome screen with the aim of identifying novel regulators of mitochondrial morphology. This screen made use of the Dharmacon siGenome siRNA library whereby 4 pooled siRNA duplexes, targeting each of 18,255 human genes, were arrayed into glass-bottom 384-well plates amenable for high-throughput imaging. HeLa cells were transfected with the arrayed siRNAs, incubated for 72h, then fixed and immunostained. Plates were scanned using the Cellomics Arrayscan vHCS, which is an automated light microscope coupled to a camera that can rapidly capture images visualized through the microscope (Figure 1a).

Images were analyzed with an algorithm generated by Dr. Stephen Baird using Cellomics image analysis software. The algorithm measures the average length:width ratio for all mitochondrial tubules from 10 fields of a given well, and assigns each well an “aspect ratio” score. The aspect ratio metric is the first unbiased quantifiable measure of mitochondrial dynamics[41]. A higher aspect ratio score denotes a more elongated mitochondrial network, whereas a lower aspect ratio score denotes a more fragmented mitochondrial network. External non-targeting siRNA and known mitochondrial morphology regulator controls were included on all plates of the screen. Mfn1/2 together were used as controls for loss of fusion (low aspect ratio), whereas Drp1 was used as a control for loss

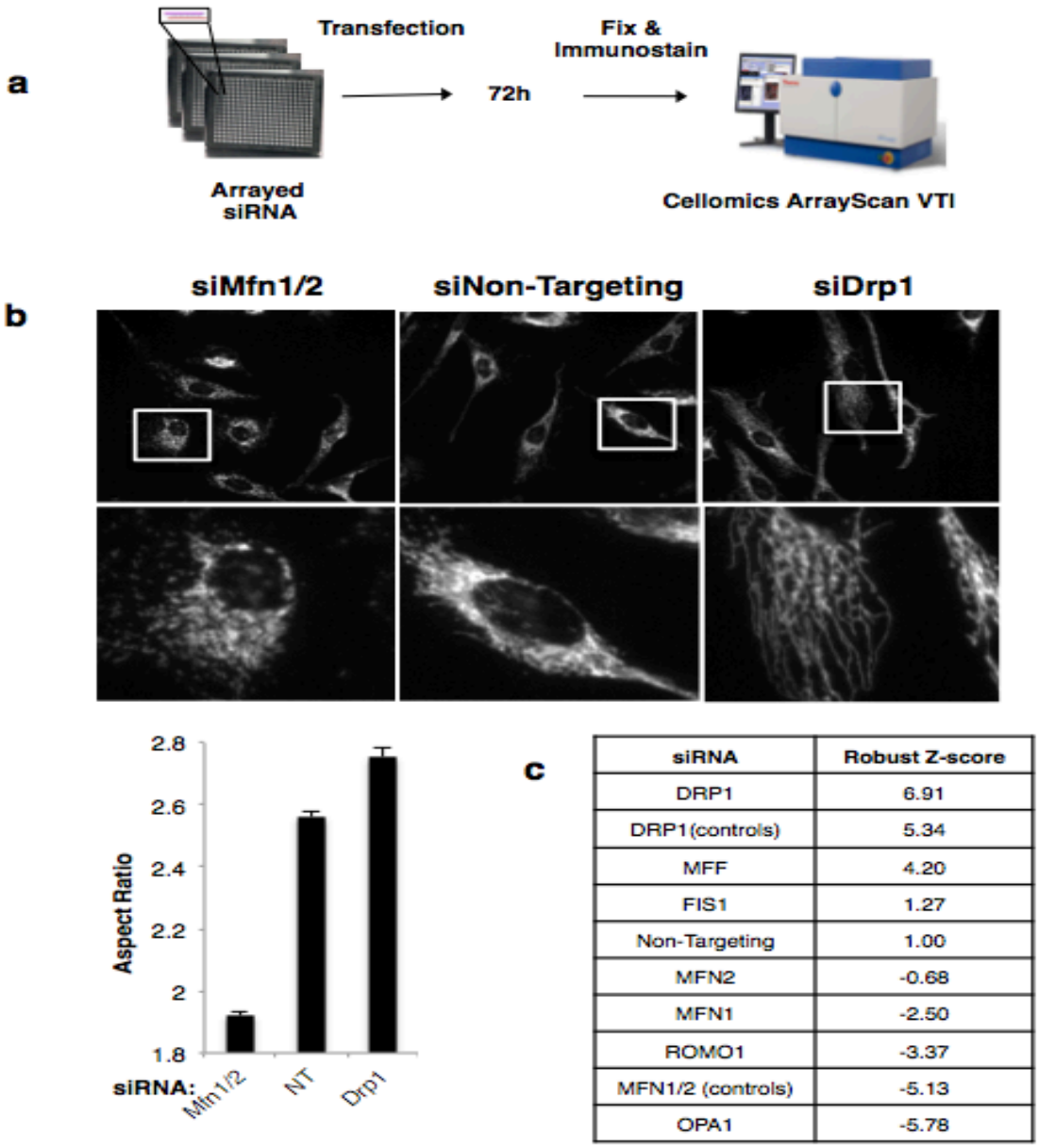

siRNA	Robust Z-score
DRP1	6.91
DRP1(controls)	5.34
MFF	4.20
FIS1	1.27
Non-Targeting	1.00
MFN2	-0.68
MFN1	-2.50
ROMO1	-3.37
MFN1/2 (controls)	-5.13
OPA1	-5.78

Figure 1. Mitochondrial Morphology Genome Screen. a. Schematic of the protocol used for the mitochondrial morphology screen. Pooled siRNA duplexes were arrayed in 384-well plate format and transfected into HeLa cells. 72h following transfection, plates were fixed and stained with Hoechst and an anti-Tomm20 antibody, to visualize nuclei and mitochondria, respectively. Plates were than imaged with the Cellomics Arrayscan automated microscope. **b. Top:** representative screen images of HeLa cells transfected with Mfn1/2 (left), Control (middle), or Drp1 (right) siRNAs. **Bottom:** screen images were quantified using an algorithm that measures the aspect ratio (length:width average) of all mitochondria in all fields of a given well. Representative aspect ratios for the aforementioned siRNA controls are shown. **c.** The median aspect ratio score from three technical replicates of the genome screen allowed a robust Z-score to be calculated for each gene. Robust Z-scores from select known regulators of mitochondrial morphology are shown.

of fission (high aspect ratio) (figure 1b). The aspect ratio of each gene was measured by 3 technical replicates, and a robust Z-score was calculated for each gene (figure 1c). Internal controls exhibited robust Z-scores >3 MADs, indicating that the screen was effectively able to separate morphological phenotypes.

Further validating the efficacy of the screen was the identification of ROMO1 as a novel regulator of IMM fusion and cristae junction integrity[41]. The discovery of ROMO1 provided convincing rational that the mitochondrial morphology screen could accurately identify novel regulators of mitochondrial dynamics, and that other candidate regulators could be identified from this screen. I therefore hypothesized that high-throughput siRNA screening would be able to identify additional novel regulators of mitochondrial morphology.

3.2 Secondary and Tertiary Screens

With the goal of identifying a novel regulator of mitochondrial dynamics, I set out to validate top candidates from the Screaton lab mitochondrial morphology screen. With deconvoluted siRNAs comprising the individual siRNA duplexes from the siRNA pools used in the original screen, I performed a secondary screen of 40 top candidate genes as assessed by their robust Z-scores (Figure 2). As no gene(s) exhibited a consistent, robust phenotype from all four siRNAs, we reasoned that using a distinct type of RNAi, shRNA, might clarify the results observed in the secondary siRNA screen. Nine genes that displayed a significant alteration in aspect ratio with 2 or more siRNAs (Figure 2, red bars) were selected for a tertiary mini-screen using shRNA (Figure 3a,b).

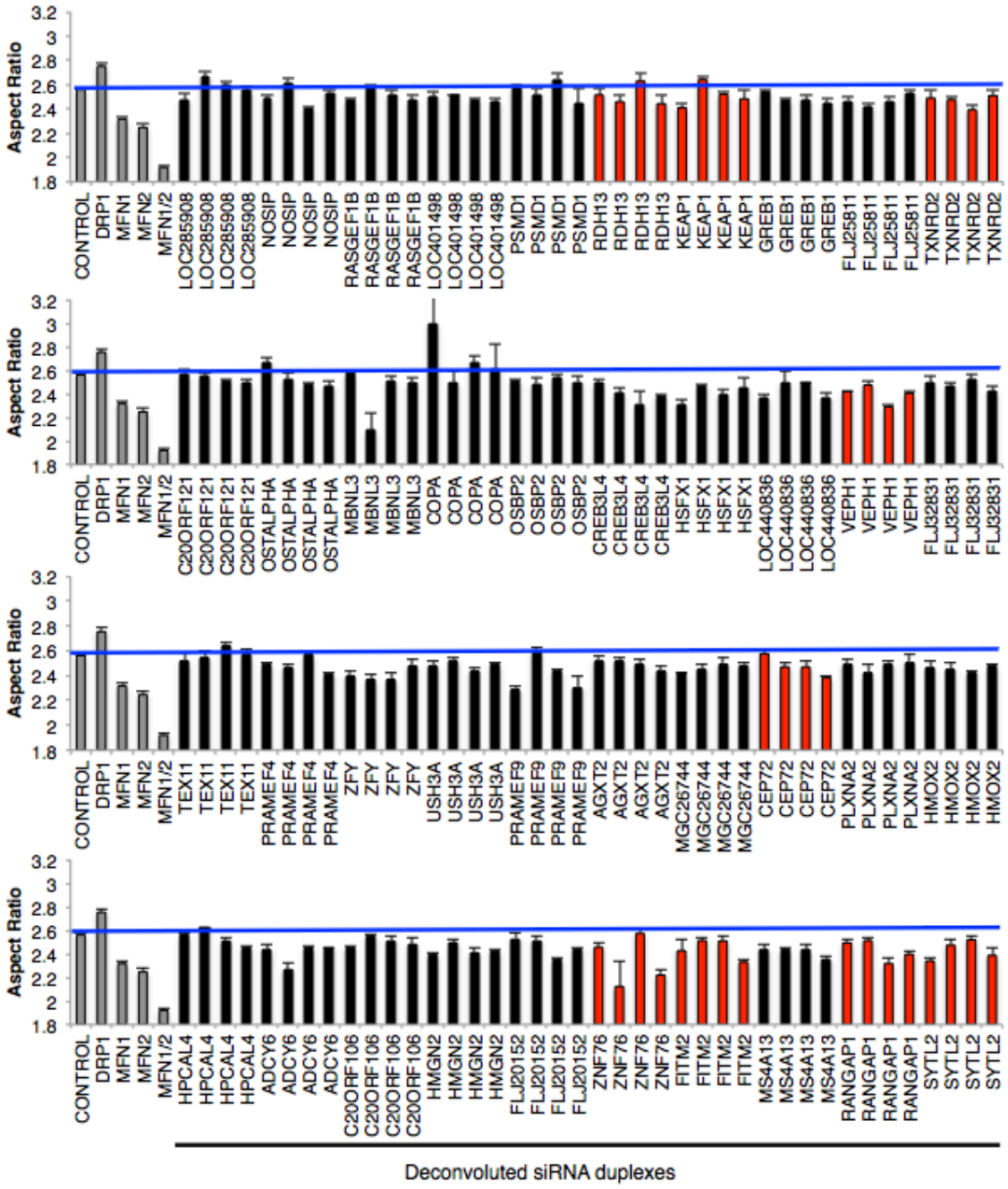

Figure 2. Secondary siRNA Screen. Four siRNA duplexes, deconvoluted from the siRNA pools used in the original genome screen, targeting each of forty genes selected based on their robust Z-scores, were arrayed in 384-well plate format. Negative control, Mfn1/2, and Drp1 siRNA were arrayed on each plate as well. Aspect ratios values represent the mean of three technical experiments. Controls (grey bars) are shown on each bar plot for clarity. Select genes that exhibited fragmentation or elongation with two or more siRNA duplexes (red bars) were selected for additional shRNA validation.

a

Letter	Gene	Gene ID	Robust Z-score
C	CEP72	55722	-3.17
R	RDH13	112724	3.76
T	TXNRD2	10587	3.58
V	VEPH1	79674	-2.93
G	RANGAP1	5905	0.51
S	SYTL2	54843	-2.39
F	FITM2	128486	-1.95
K	KEAP1	9817	3.62
Z	ZNF76	7629	-3.91

b

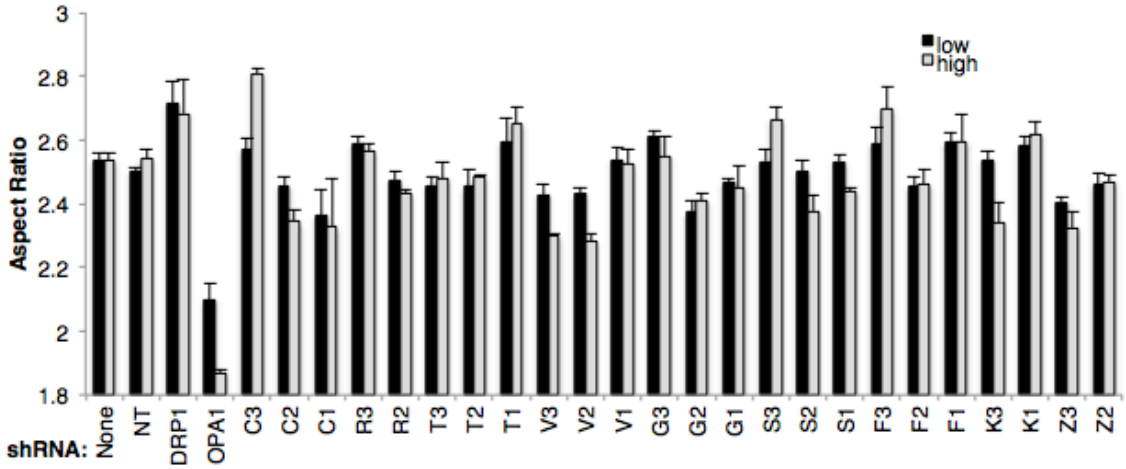

Figure 3. Secondary shRNA Screen. a. Nine genes were selected for shRNA validation based on their phenotypes from the deconvoluted siRNA screen. Robust Z-scores from the original screen are included. **b.** Three distinct shRNAs, arbitrarily labeled 3-1, were designed and generated against each of the nine genes in panel a. HeLa cells were seeded in a 384-well plate and infected with low and high concentrations of lentivirus carrying each shRNA. 72h following infection, mitochondrial morphologies were quantified. Aspect ratios reflect the mean of three independent experiments.

Two of three shRNAs targeting the gene, VEPH1 (ventricular zone expressed PH domain-containing 1), elicited fragmentation of the mitochondrial network in a lentiviral dose-dependent manner (Figure 4a), which was confirmed visually (Figure 4b). VEPH1 had a robust Z-score of -2.93 from the initial screen, as well as all siRNA duplexes elicited mild fragmentation in the deconvoluted screen (Figure 2), providing correlative evidence that VEPH1 was involved in regulating mitochondrial morphology. VEPH1-sh3 targets the 3' UTR of the VEPH1 transcript and therefore does not target VEPH1 mRNA transcribed from a plasmid containing the VEPH1 gene cloned from cDNA. Reintroduction of VEPH1 into cells infected with VEPH1-sh3 was unable to restore mitochondrial morphology (figure 4c), suggesting that the fragmentation phenotype elicited by VEPH1 shRNAs was due to off-target effects. An antibody against VEPH1 was unable to detect the predicted VEPH1 species by Western blot and therefore, I could not validate that VEPH1 sh2 or sh3 truly knocked down VEPH1. As the fragmentation phenotype could not be rescued by reconstitution of VEPH1, nor could any of the RNAi reagents be validated for function, I did not proceed further with trying to validate VEPH1 as a novel regulator of mitochondrial dynamics.

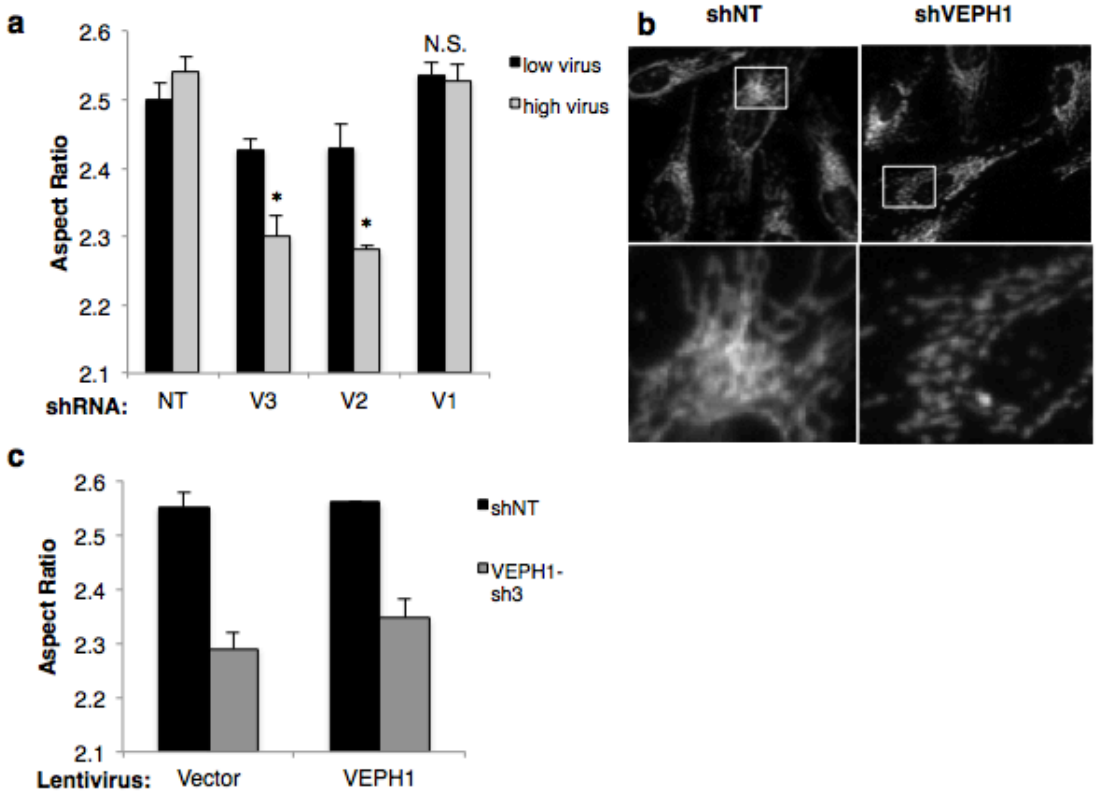

Figure 4. VEPH1 Does Not Regulate Mitochondrial Morphology. a. HeLa cells infected with shRNAs targeting VEPH1 (described in figure 3) display a dose-responsive reduction in aspect ratio with 2 of 3 shRNAs targeting VEPH1 (*=P<0.05, N.S. = not statistically significant). **b.** HeLa cells infected with VEPH1 shRNA display a fragmented mitochondrial network as compared with cells infected with non-targeting shRNA. Images were captured with the Cellomics automated microscope and are representative of 10 individual fields. **c.** Lentiviral expression of VEPH1 is unable to restore mitochondrial morphology in VEPH1 KD cells. Unsuccessful rescue results are representative of three independent experiments.

3.3 Informed Candidate Validation

Having had little success with unbiased validation of candidate regulators of mitochondrial dynamics, we elected to next take a more informed approach to candidate selection. A collaborator, Dr. Miguel Andrade of the Johannes Gutenberg University in Germany, performed a bioinformatic analysis to identify select genes that were predicted to be localized to both mitochondria and the endoplasmic reticulum (ER) on the basis of *in silico* targeting sequence predictions and existing literature. It has been previously demonstrated that ER tubules dictate sites of mitochondrial division in part by physically constricting the mitochondrion to a diameter more amenable to DRP1 oligomerization[47]. We reasoned that there might be additional unknown regulatory proteins involved in ER-contact mediated mitochondrial division. Andy Ng and I began cloning genes from the list provided by Dr. Andrade, fusing each of them with GFP at the N or C terminus. For the genes that we were able to clone, we generated lentivirus, and infected U2OS cells stably expressing the ER-marker fusion protein, Sec61β-mcherry. We then immunostained the cells for the mitochondrial marker, Tomm20, and looked for genes where the GFP signal localized with both the ER and Tomm20 signal (Figure 5a). One gene in particular, C18ORF32 (LOC497661), displayed both ER and mitochondrial localization as observed by GFP signal (Figure 5b). C18ORF32 also obtained a robust Z-score of 3.06 from the initial genome screen, indicating that loss of this gene significantly elongated the mitochondrial network. Taken together, the ER-mitochondria localization and

a

Gene Name	Gene ID	Robust Z score (screen)	Predicted Loca-lization	GFP-Gene	Gene-GFP
CHST9	83539	3.24	ER	No signal	ER, with some cells displaying GFP in the golgi
UBE2J1	51465	3.19	ER	ER	ER
C18orf32 (LOC497661)	497661	3.06	ER	No signal	**ER and mitochondria**
YKT6	10652	2.78	Mitochondria	Cytoplasmic with some punctate mitochondrial signal	Expressed throughout the entire cell
SRP14	6727	2.70	Cytoplasm	No signal	Nuclear and nucelolar

b

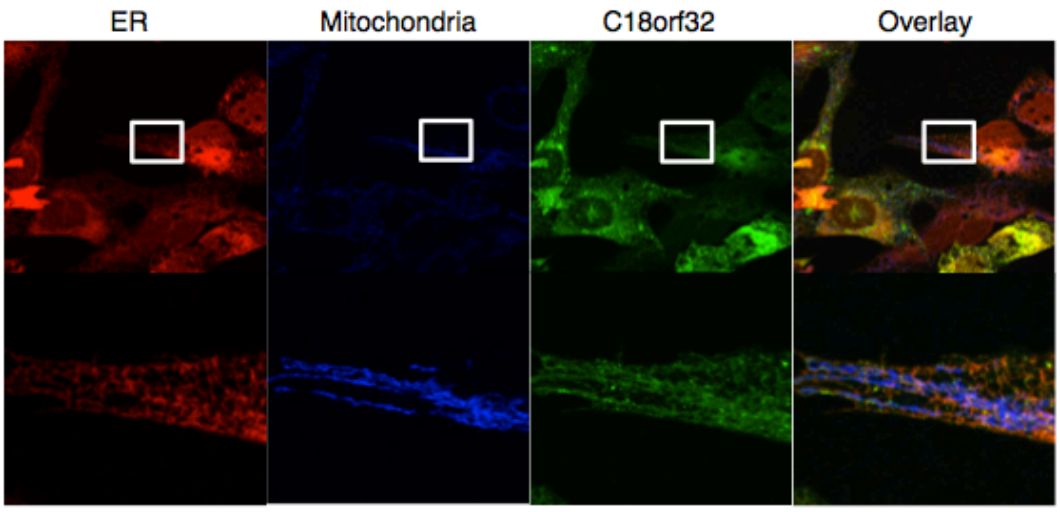

Figure 5. Identification of C18ORF32 as a Candidate Modulator of Mitochondrial Fission. a. Genes predicted to be associated with the ER that had significant positive robust Z-scores were cloned and fused to GFP at the N or C terminal. U2OS cells stably expressing the ER-marker, Sec61β, were infected with lentivirus expressing the GFP-fusion fusion genes. 72h following infection, cells were fixed and stained for mitochondria with an antibody against Tomm20, then analyzed by confocal microscopy for genes where GFP signal co-localized with both the ER and mitochondria. Select observations are recorded. **b.** C18ORF32-GFP, displayed significant ER co-localization, as well as mitochondrial overlap, suggesting that this gene associates with both organelles and is a promising regulator of mitochondrial fission. Images captured with the 40X objective of the Olympus Fluoview confocal microscope.

robust Z-score suggested that C18ORF32 was a promising candidate regulator of mitochondrial fission.

Introduction of one siRNA from the deconvoluted pool targeting C18ORF32, resulted in dramatic elongation of the mitochondrial network in U2OS cells (Figure 6a). This same siRNA produced significant elongation, and two other siRNAs produced mild elongation of the mitochondrial network by aspect ratio measurement (Figure 6b). Knockdown of C18ORF32 protein level was confirmed by WB with an antibody against C18ORF32. Neither knockdown nor overexpression of C18ORF32 had an observable effect on the levels of known regulators of mitochondrial dynamics (Figure 6c). In order to monitor expression levels of C18ORF32 during rescue experiments, I generated an siRNA-resistant C18ORF32 construct fused to a C-terminal V5 tag (the antibody against C18ORF32 was not suitable for IF). Reintroduction of C18ORF32-V5 into cells lacking C18ORF32 did not restore morphology to control levels, however I noticed that introduction of the V5-tagged cDNA significantly elongated the mitochondrial network under control conditions (Figure 6d). This observation raised the possibility that the V5 tag was interfering with C18ORF32 function making the protein a dominant-negative, so future rescue experiments were performed using an untagged C18ORF32 cDNA.

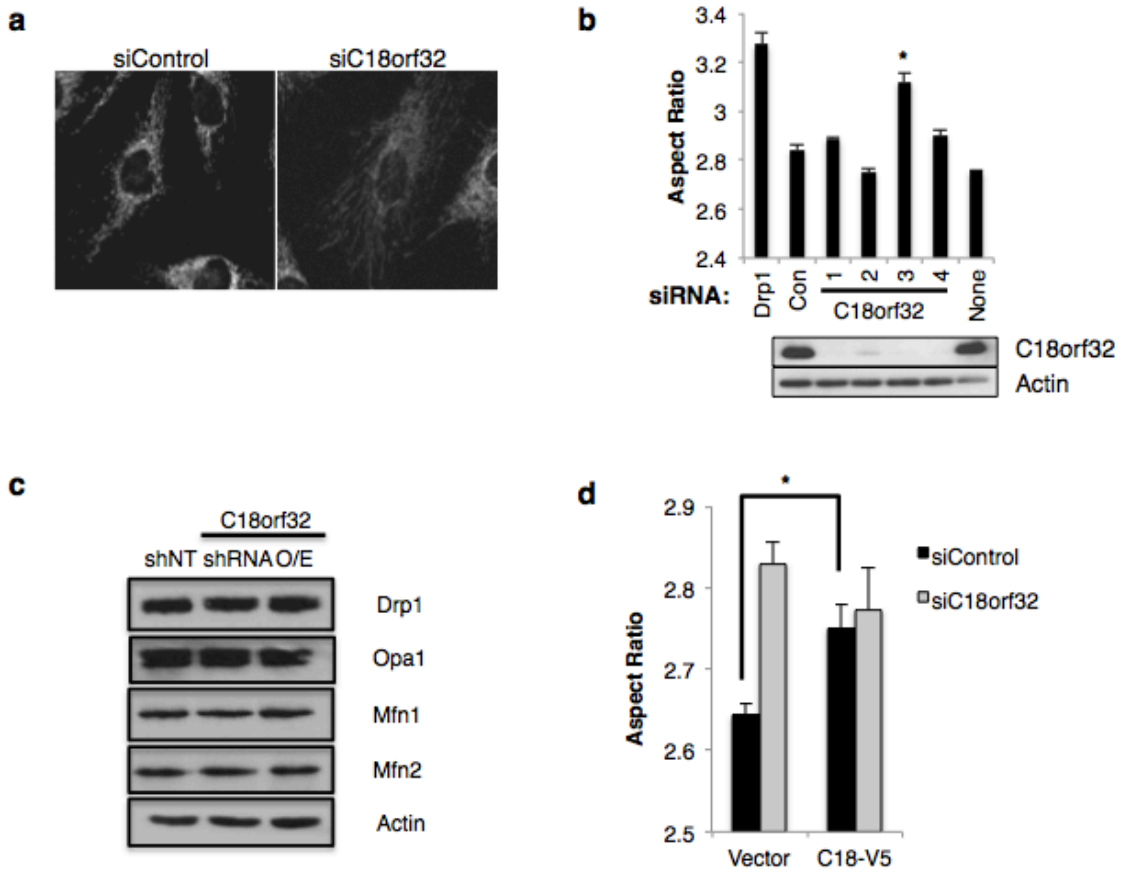

Figure 6. KD of C18ORF32 Elongates the Mitochondrial Network. a. U2OS cells transfected with siRNA targeting C18ORF32 display an elongated mitochondrial network compared with control. Representative fields of images captured by Cellomics are shown. **b.** All 4 siRNAs targeting C18ORF32 can functionally knock it down at the protein level. Only si3 elicits dramatic elongation (*=P<0.05), whereas si1 and si4 elicit mild elongation of the mitochondrial network (N.S.). **c.** U2OS cells infected for 72h with lentivirus expressing either a C18ORF32 cDNA or an shRNA targeting C18ORF32 display no change in protein levels of known regulators of mitochondrial fusion of fission: MFN1, MFN2, OPA1, or DRP1. **d.** Introduction of an siRNA-resistant C18ORF32-V5 construct into cells transiently lacking C18ORF32 (transfected with si3) does not rescue mitochondrial morphology. Rather, introduction of the C18ORF32-V5 construct is sufficient to significantly elongate the mitochondrial network (*=P<0.05).

Titration of increasing amounts of C18ORF32 was unable to restore normal mitochondrial morphology in cells transiently lacking C18ORF32 (Figure 7a). We reasoned that infection and expression heterogeneity were possible explanations as to why C18ORF32 could not rescue basal mitochondrial morphology. Using C18ORF32-V5 as a proxy for untagged C18ORF32 infection and expression, I demonstrated that at protein levels far exceeding endogenous (Figure 7b), V5 expression was very heterogeneous and only present in a subset of cells (Figure 7c). As overexpression of an untagged protein is also reported to exert dominant negative effects[69, 71], there was no way to conclusively validate C18ORF32 as a regulator of mitochondrial dynamics. Despite convincing lines of evidence suggesting C18ORF32 might play a role in mitochondrial dynamics, we decided to discontinue validation of it as a candidate.

3.4 Genome Screen Repeat Identifies MTX2 as a Novel Regulator of Mitochondrial Dynamics

Having been unable to rescue several promising candidates, we decided to re-evaluate the follow-up protocol that we used to validate candidates from the mitochondrial morphology screen. A general consensus between Dr. Screaton, other graduate students working on mitochondrial dynamics projects, and I, was that we were focusing on too many false positives as a result of ambiguous screen data. The phenotypes of most known regulators of mitochondrial dynamics could be easily quantified from Cellomics screen images, however milder phenotypes could be missed from a lack of image resolution and algorithm

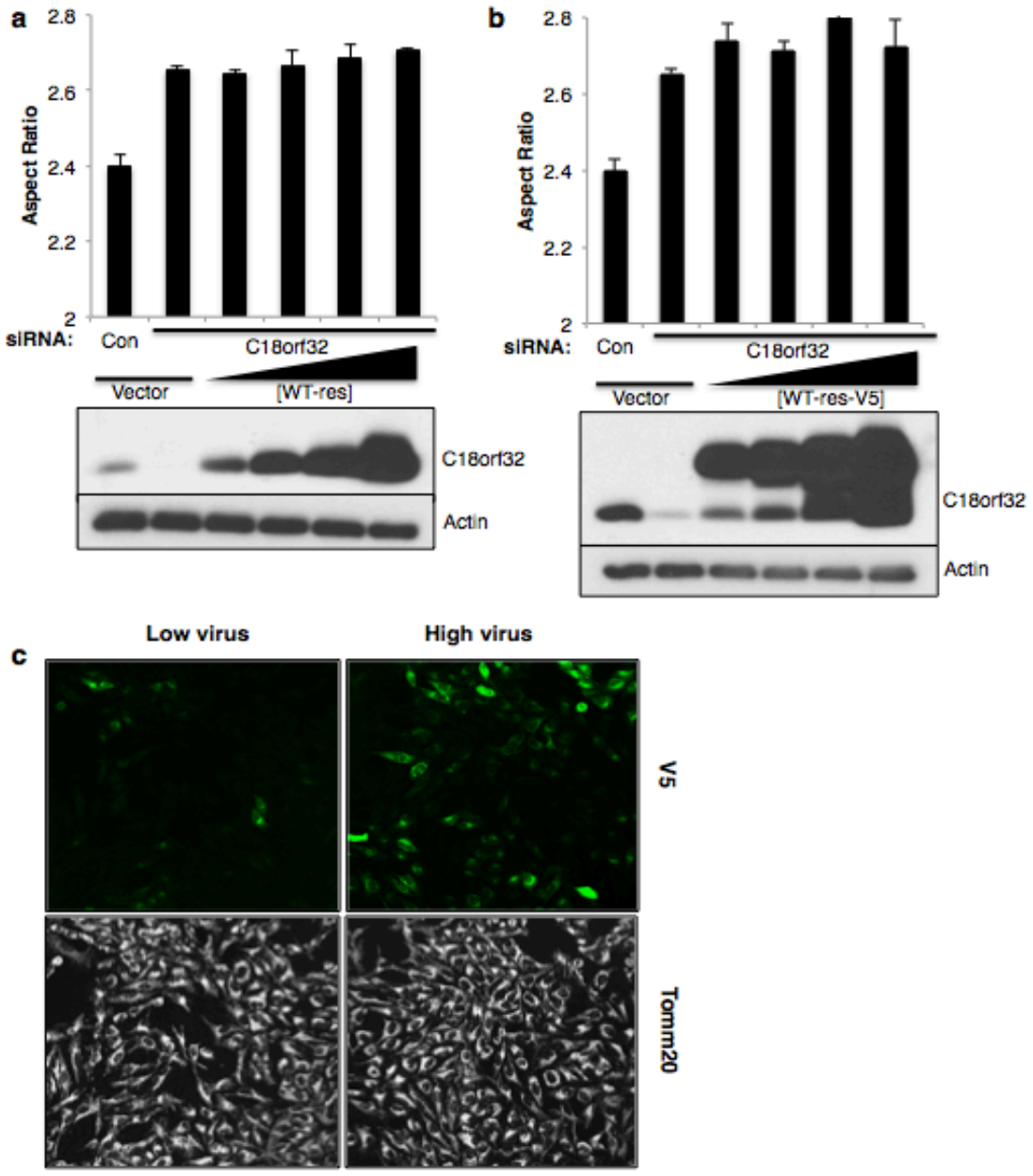

Figure 7. Overexpression of C18ORF32 Does Not Restore Basal Mitochondrial Morphology. a. Titration of increasing concentration of lentivirus expressing an siRNA-resistant C18ORF32 construct was unable to restore basal mitochondrial morphology in U2OS cells transiently lacking C18ORF32. **b.** U2OS cells were similarly infected with siRNA-resistant C18ORF32-V5, which was also unable to rescue basal mitochondrial morphology. **c.** Fixed cells from the experiment in panels a and b were incubated with an antibody against V5, and analyzed by confocal microscopy. Even at the lowest level of virus, (panel b, 3rd lane from the left) overexpressed C18ORF32 levels far exceed basal C18ORF32 levels (panel b, 1st lane), whereas V5 signal is barely detectable (panel c, top left). V5 signal is used as a proxy for untagged C18ORF32 expression. For WB, cells were lysed and protein was pooled from 6 wells of a 384-well plate transfected in parallel to the plate used for aspect ratio analysis in order to control for transfection efficiency in 384-well format.

limitations. As such we decided to repeat the genome screen, using the Opera automated confocal microscope to perform the cellular imaging analysis to improve image resolution. Andy Ng and I carried out the genome screen, and quantitation of the screen results is ongoing (May 2014).

In the meantime, I developed a list of mitochondrially-associated genes based on the Broad Institute's Mitocarta database (http://www.broadinstitute.org/pubs/MitoCarta/; a list of murine genes and their human homologues as assessed by mass spectrometry on isolated mitochondria from 14 mouse tissues) (Figure 8a). Qualitative analysis of screen images for all genes in the candidate list identified three promising candidate regulators of mitochondrial dynamics (Figure 8b). Deconvolution of siRNA pools targeting these three genes demonstrated that 4/4 siRNAs targeting Metaxin 2 (MTX2) knocked down the protein and resulted in a significant fragmentation phenotype (Figure 9a). There was no correlation between knockdown and phenotype with GHITM (Figure 9b) or MMACHC (Figure 9c), so these candidates were removed from further validation experiments.

Reconstitution of an MTX2 construct (resistant to siRNAs 2 and 3 targeting MTX2) into MTX2 knockdown cells was able to partially restore mitochondrial morphology (Figure 10a, Supp. Fig. 1). This rescue was observed with both siRNAs 2 and 3 targeting MTX2, as well as with a C-terminal V5-tagged siRNA-resistant MTX2 construct, indicating that this construct retains its function despite the V5-tag. Interestingly, expression of MTX2-V5 results in an-upward shifted

a

Gene	Gene Description	Synonyms	Gene ID	Plate ID	Observations	have deconvoluted reagents/Found in a 2ndary set
TMEM11	transmembrane protein 1	C17orf35, PMI, PMI	8834	01-B16	Cell Death/ no phenotype (029)	* = multiple coordinates
NME3	non-metastatic cells 3, pr	DR-nm23, KIAA0516	4832	02-K11	possible elongation, may be starting to fragment (029); no phenotype (030)	
FASTK	Fas-activated serine/thre	FAST	10922	02-K22	No phenotype (029)	
PINK1	PTEN induced putative k	BRPK, FLJ27236, PA	65018	03-B12	Big networks, mildly fragmented on their exteriors (029); fairly fragmented (030)	
FXN	frataxin	CyaY, FA, FARR, FR	2395	03-E13	No phenotype (029)	
NME1	non-metastatic cells 1, pr	AWD, GAAD, NDPK	4830	03-F15	No phenotype (029)	
ADCK4	aarF domain containing k	COQ8, FLJ12229	79934	03-H09	No phenotype (029)	
ADCK2	aarF domain containing k	AARF, MGC20727	90956	03-K06	Some elongation (029); mild elongation (030)	
NME4	non-metastatic cells 4, pr	NM23H4, nm23-H4	4833	04-K10	very mild fragmentation/ no phentoype (029)	
C10orf89	chromosome 10 open rea	MGC35392, PSTK	118672	04-L11	No phenotype (029)	
YME1L1	YME1-like 1 (S. cerevisi	PTSH, MEG4, PAMP	10730	05-C18	No phenotype (029)	
CLPP	ClpP caseinolytic peptida	N/A	8192	05-D22	No phenotype (029)	
PITRM1	pitrilysin metallopeptidas	KIAA1104, MGC138	10531	05-H07	very long, thin cells, but not necessarily elongated (029); same (030)	
LONP1	lon peptidase 1, mitochor	LON, LONP, LonHS,	9361	05-I14	No phenotype (029)	
OSGEPL1	O-sialoglycoprotein endo	N/A	64172	05-I22	Some condensation of the network, but no real phenotype (029); No phenotype (030)	
PRSS35	protease, serine, 35	C6orf158, MGC4652	167681	05-K20	very long, thin cells, but not necessarily elongated (029); same (030)	
CASP8	caspase 8, apoptosis-relat	CAP4, FLICE, MACI	841	05-N08	Elongation, with some network condensation (029); maybe elongation/No phenotype (030)	
CLPX	ClpX caseinolytic peptida	N/A	10845	05-N13	very long, thin cells, with some elongation (029); long cells, Elongation (030)	
IMMP2L	IMP2 inner mitochondria	IMP2	83943	06-C03	No phenotype (029)	
AFG3L2	AFG3 ATPase family ger	FLJ25993	10939	06-D21	small, thin cells, No phenotype (029)	
OMA1	OMA1 homolog, zinc me	2010001O09Rik, DAI	115209	06-F03	some fragmentation at the exterior of networks (029); same, some condensation of the network (030)	
MIPEP	mitochondrial intermedia	HMIP, MIP	4285	06-F16	No phenotype (029)	
NLN	neurolysin (metallopeptic	AGTBP, DKFZp564F	57486	06-N04	small, thin cells, No phenotype (029)	
TOMM40	translocase of outer mito	C19orf1, D19S1177E	10452	07-B21	No phenotype; mild fragmentation (029)	
TSPO	translocator protein (18kI	BZRP, DBI, IBP, MBI	706	07-D13	No phenotype (029-images were overexposed)	
VDAC3	voltage-dependent anion	HD-VDAC3	7419	07-D22	very long, thin cells, but not necessarily elongated (029);	
VDAC2	voltage-dependent anion	FLJ23841	7417	07-E12	Fragmentation in half the cells, others long and skinny or no phenotype (029); same, possibly more fragmented (	
VDAC1	voltage-dependent anion	MGC111064, PORIN	7416	07-K06	No phenotype (029); mild fragmentation (030)	
C6orf49	chromosome 6 open read	MGC120398, OBTP,	29964	08-B20	No phenotype (029)	
C1orf166	chromosome 1 open read	FLJ12875, RP11-401	79594	09-J10	Very condensed networks, mild fragmentation (029); same, possibly cell death (030)	
GLRX2	glutaredoxin 2	GRX2, hA101E13.1	51022	10-G19	No phenotype; some skinny cells (029)	

b

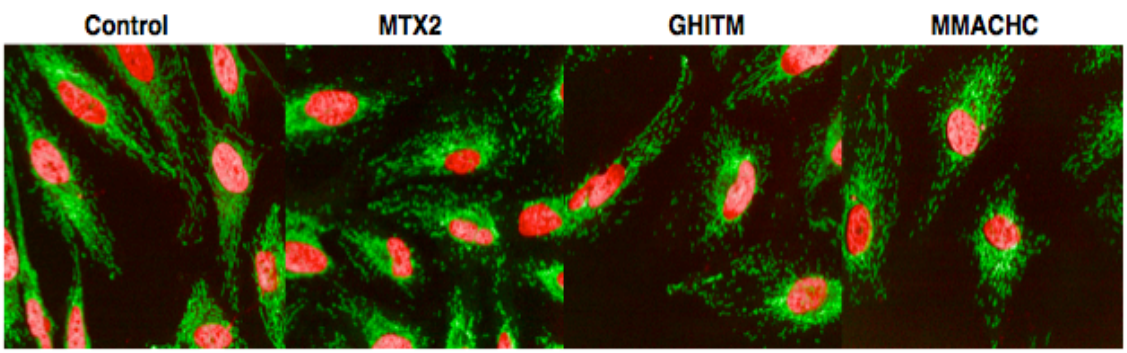

Figure 8. Identification of Candidates from the Genome Screen Repeat. a. Schematic of the shortlist of genes to be assessed visually for their effect on mitochondrial morphology. Images from 42 fields of each gene from the genome screen repeat were analyzed visually and observations were recorded (6th column). If KD of a gene appeared to result in a mitochondrial morphological phenotype, that well was assessed visually from a technical replicate plate to confirm the observed phenotype. Mitochondrial morphology controls were assessed visually on each plate to ensure that siRNA transfection had worked. Knockdown of 3 genes: MTX2, GHITM, and MMACHC, resulted in significant fragmentation of the mitochondrial network, as observed qualitatively. **b.** Representative screen images demonstrating: Control, MTX2, GHITM, and MMACHC morphologies (left to right).

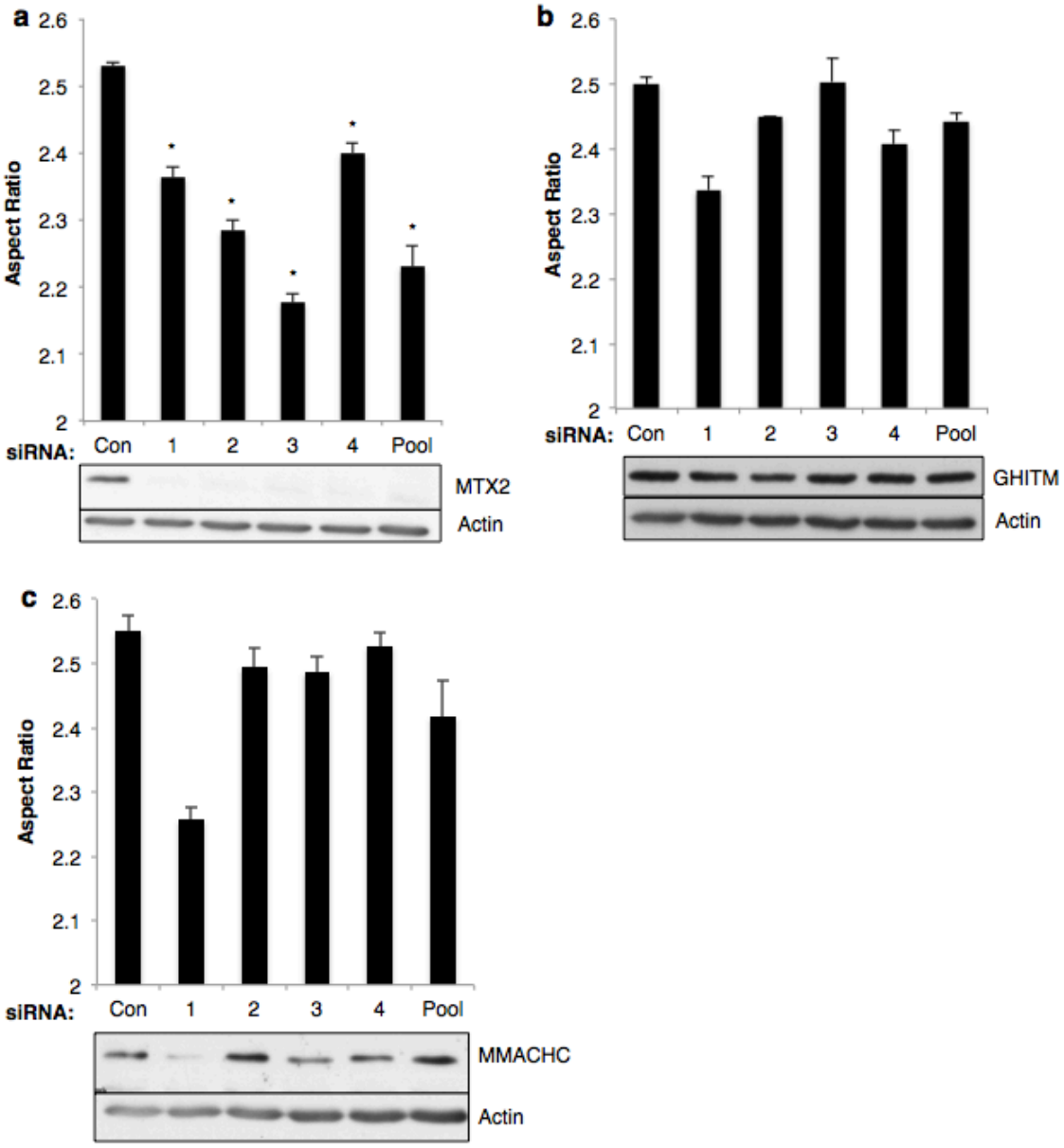

Figure 9. MTX2 Displays Correlation Between Knockdown and Phenotype. HeLa cells were transfected with deconvoluted siRNAs corresponding to the siRNA pool used in the genome screen. **a.** All siRNAs targeting MTX2 elicit significant fragmentation of the mitochondrial network, while ablating MTX2 protein levels (*=P<0.05). **b.** GHITM protein levels were maintained in the presence of siRNAs targeting this gene, suggesting phenotypic effects were 'off-target'. **c.** Tenuous correlation between KD and phenotype for MMACHC, suggesting phenotypic effects were 'off-target'. For WB, cells were lysed and protein was pooled from 6 wells of a 384-well plate transfected in parallel to the plate used for aspect ratio analysis in order to control for transfection efficiency in 384-well format. MTX2 aspect ratio and knockdown WB are representative of 3 independent experiments.

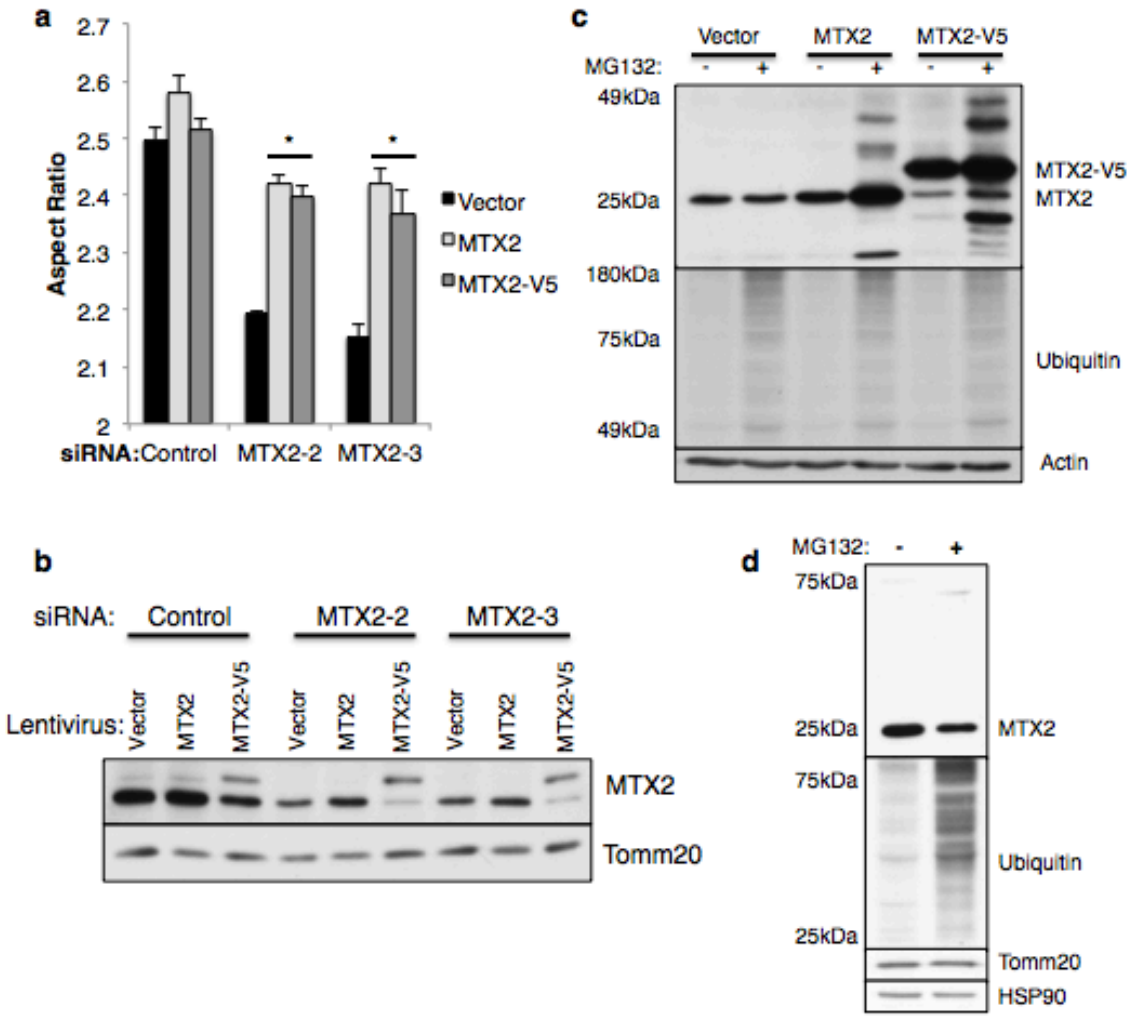

Figure 10. MTX2 Regulates Mitochondrial Morphology, While It is Tightly Regulated. a. Reintroduction of an siRNA-resistant MTX2 construct into HeLa cells transiently lacking MTX2 results in partial restoration of mitochondrial morphology. Two individual siRNA duplexes were both rescued by reintroduction of MTX2, as well as MTX2-V5 (*=P<0.05 comparing [siMTX2+Vector] to [siMTX2+MTX2]). Rescue quantification is representative of three independent experiments. **b**. For WB, cells were lysed and protein was pooled from 6 wells of a 384-well plate transfected in parallel to the plate used for aspect ratio analysis in order to control for transfection efficiency in 384-well format. **c.** U2OS cells were infected with lentivirus expressing: vector, MTX2, or MTX2-V5 for 72h, then treated with 10uM MG132 for 8h, before being harvested. Overexpressed MTX2(-V5) accumulates in the presence of MG132. Total ubiquitin serves as a positive control for MG132 treatment. WB is representative of 2 independent experiments. **d.** HeLa cells were incubated for 72h, then treated with 5uM MG132 for 24h before being harvested. There is no accumulation of endogenous MTX2 levels even after 24h of proteasome inhibition.

species corresponding to V5-tagged MTX2 on a Western blot (Supp. Fig. 2), which accumulates at the expense of endogenous MTX2 levels (Figure 10b). The idea that endogenous MTX2 is lost in response to MTX2 overexpression suggests that MTX2 levels are tightly regulated by the cell. To investigate the mechanism of MTX2 regulation, I infected U2OS cells with lentivirus expressing MTX2 for 72h, then treated the cells with the proteasome inhibitor MG132. MG132-treated cells display an accumulation of both MTX2, as well as higher molecular weight species, likely corresponding to ubiquitinated MTX2 (Figure 10c). Interestingly, no accumulation of endogenous MTX2 is observed even after 24h of MG132 treatment (Figure 10d).

Knockdown of MTX2 had no observable effect on levels of DRP1, MFN1, or MFN2 (Figure 11a). By Western blot, there was a minor accumulation of OPA1 isoform C, which, along with loss of long OPA1 isoforms, was more dramatic in U2OS cells (Figure 11b). The loss of OPA1 long isoforms is consistent with mitochondrial network fragmentation and cristae remodeling observed prior to apoptosis. MTX2 knockdown did not affect mitochondrial membrane potential though (Supp. Fig. 3). Contrary to others' observations that fragmentation sensitizes cells to tBid-induced cytochrome C release[76], MTX2 knockdown actually blunts cytochrome C release rather than sensitizes cells to it (Figure 11c). This interesting finding raises the possibility that MTX2 has dual roles in regulating both mitochondrial morphology and apoptosis.

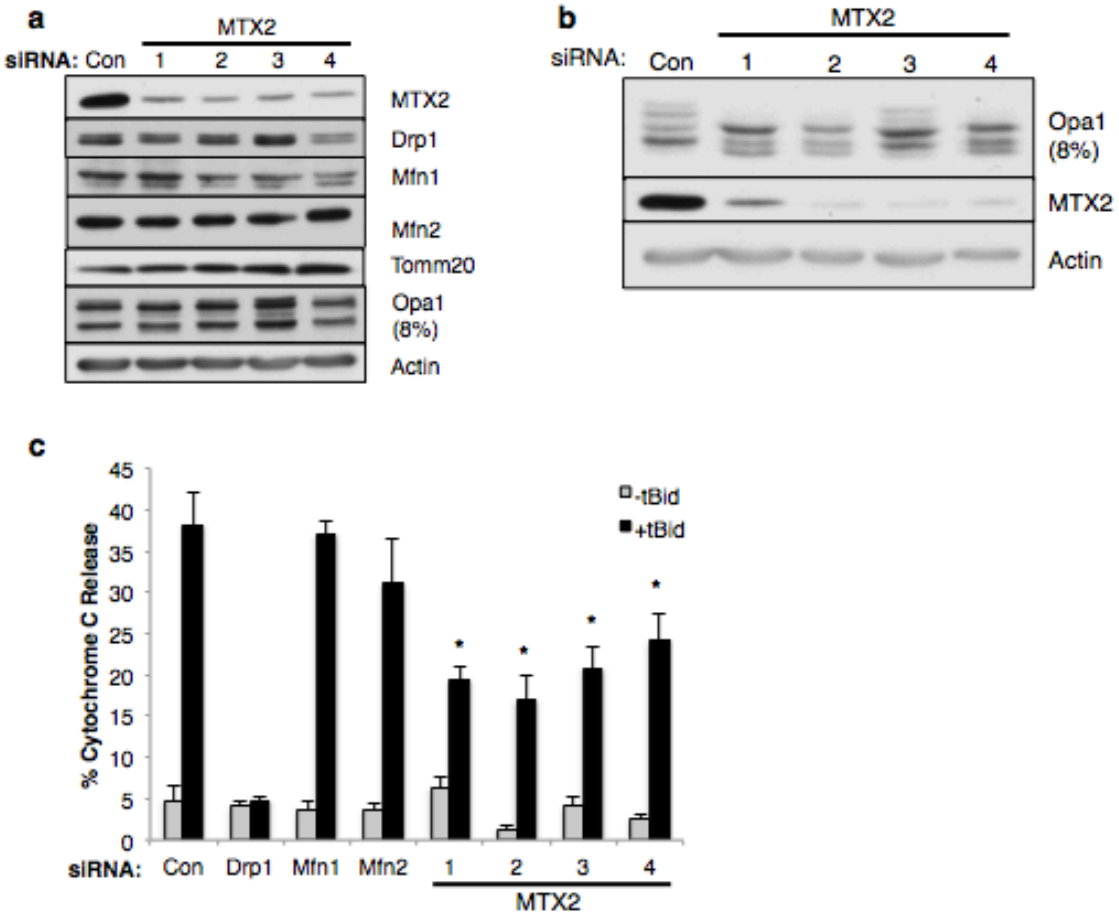

Figure 11. MTX2 KD Affects Opa1 Isoform Balance and Blunts Apoptosis. a. Protein from HeLa cells, transfected with MTX2 siRNAs for 72h, was harvested and resolved by SDS PAGE. WB analysis shows no difference in MFN1, MFN2, or DRP1 levels following MTX2 KD. OPA1 isoform C accumulates following MTX2 KD. **b.** U2OS cells display a loss of long OPA1 isoforms and an accumulation of short OPA1 isoforms following MTX2 KD. OPA1 WBs are representative of 3 independent experiments and were resolved for 1:15h in 8% polyacrylamide. **c.** 72h following transfection as described in panel a, HeLa cells were treated with doxycycline, QVD, and adenovirus carrying inducible truncated BID (tBID) to induce apoptosis. After 4h of tBID treatment, cells were fixed and immunostained for mitochondria and cytochrome C, then analyzed with a colocalization algorithm that quantifies the amount of cytochrome C retained in mitochondria. MTX2 knockdown desensitizes cells to cytochrome C release relative to control siRNA (*=P<0.1). Desensitization to cytochrome C release has been observed in 3 independent experiments.

Chapter 4. Discussion

4.1 Failed Candidate Validation

Genome screens are powerful tools for identifying novel regulators of critical biological processes. Unfortunately, in the case of RNAi screens, the prevalence of OTEs result in an arduous process required to validate candidates as true positives. The gold standard for validating a candidate as a true positive is genetic rescue via reintroduction of an siRNA-resistant cDNA into cells transfected with siRNA targeting that gene. Rescue experiments themselves are a long process with their own caveats, so prior to rescue a secondary validation whereby multiple RNAi reagents are shown to elicit the same phenotype is usually recommended.

4.1.1 VEPH1

VEPH1 was originally selected for secondary validation based on a robust Z-score of -2.93, which indicated that its knockdown resulted in significant mitochondrial network fragmentation. Four deconvoluted siRNAs targeting VEPH1 all elicited very mild fragmentation. We reasoned that the siRNA duplexes might be less effective individually, compared with when they were pooled together, so we continued validating VEPH1 despite the mild deconvolution phenotype. Treatment of cells with shRNA targeting VEPH1 resulted in mitochondrial network fragmentation in a dose-dependent manner, which suggested that the phenotype elicited by RNAi was not a result of OTEs[144]. An antibody against VEPH1 did not detect a species of the predicted

molecular weight by WB, so I was unable to formally verify a correlation between VEPH1 protein levels and knockdown. An inability to assess VEPH1 levels was an issue when trying to rescue VEPH1. We have observed a common difficulty of lentiviral overexpression to be heterogeneous in infection and expression of the gene within the cell population. I could monitor VEPH1-GFP expression, however it was likely that the exogenous fusion protein was being expressed to many times the level of the endogenous protein in only a sub-population of cells. Several attempts to rescue the fragmentation phenotype produced by VEPH1 shRNAs proved unsuccessful. Because I could not formally verify that VEPH1 was knocked down by siRNA or shRNA, nor could VEPH1 reconstitution rescue the fragmentation phenotype, there was no rational to continue with this gene as a candidate.

4.1.2 C18ORF32

C18ORF32 was selected from a small list of predicted ER/Mitochondrial-associated genes, and colocalization with both the ER and mitochondria was observed by immunofluorescence. Additionally, C18ORF32 had a robust Z-score of 3.06 from the original screen, which taken together, provided us with strong rational to follow up on C18ORF32 as a mediator of mitochondrial fission. All four deconvoluted siRNAs knocked down C18ORF32 at the protein level, however two produced very mild elongation, and only one produced significant elongation, as quantified by aspect ratio. Despite the lack of correlation between knockdown and phenotype, we decided to continue validating C18ORF32 as a candidate due

to the convincing preliminary data suggesting it had a role in mediating mitochondrial fission. Lentiviral expression of a C-terminal V5-tagged siRNA-resistant C18ORF32 cDNA was unable to rescue mitochondrial elongation, and instead actually resulted in elongation. Given reported overexpression artifacts, for example the MiD proteins[69, 71], we reasoned that achieving endogenous expression levels of C18ORF32 was critical to its successful rescue. Following multiple unsuccessful attempts in different cell lines, it became apparent that an insurmountable challenge would be achieving homogeneous expression of C18ORF32 in a cell population. Even at barely detectable levels by immunofluorescence (Figure 7c), C18ORF32 protein levels were higher than endogenous (Figure 7b). I was unable to rescue C18ORF32 knockdown morphology, however, given the potential of overexpressed C18ORF32 functioning as a dominant-negative, I did not formally disprove it as a regulator of mitochondrial dynamics either.

4.1.3 Functional Correlation

In retrospect, the biggest red flag against VEPH1 and C18ORF32 should have been a lack of correlation between knockdown and phenotype. Numerous functional observations suggested a role for C18ORF32 in mitochondrial dynamics (ER-mitochondrial localization; mitochondrial network elongation with both knockdown and overexpression). Nonetheless, knockdown did not correlate with phenotype indicating that despite convincing biology, C18ORF32 is most likely not involved in regulating mitochondrial morphology. If a phenotype is real

(i.e. caused by knockdown of the target gene and not OTEs), then it will be observed whenever the gene is knocked down, whereas there should be no phenotype if protein levels of that gene persist[144]. If any siRNA duplex knocks down the protein and does not exhibit a phenotype, or does not knockdown the protein but induces a phenotype, OTEs must be considered. In theory, partial knockdown of a protein should result in a partial phenotype, whereby a dose-response to increasing concentrations of si/shRNA suggests that the effects are on target[141]. This approach is accompanied by the caveat that protein activity does not necessarily always correlate with protein level, for example proteins with enzymatic activity, where 10% of endogenous protein can account for 50% of endogenous enzymatic activity. It has been my experience that correlation between knockdown and phenotype is the best way to account for OTEs and identify true positives from a secondary siRNA screen.

Correlation of knockdown and phenotype is not necessarily a viable means of validating candidates from all genome screens, as it requires a functional antibody or reliable QPCR data, making it difficult for certain genes (membrane bound, or highly conserved in other species), as well as impractical for large secondary sets of candidates. Under appropriate circumstances though, correlation between knockdown and phenotype (with multiple functional RNAi reagents) is the best method of validating a secondary screen candidate, preceding genetic rescue.

4.2 Repeating the Genome Screen

The main reason for repeating the genome screen stemmed from an overall inability of several Screaton lab personnel to successfully validate novel regulators of mitochondrial dynamics using original screen data. As validation of candidates is a time-consuming and expensive process, it was vital that a reliable list of candidates was used for secondary follow up experiments. After secondary deconvolution screening of over 150 genes identified only ROMO1 as a regulator of mitochondrial dynamics, we decided that it would be less expensive and more efficient to repeat the genome screen with a confocal microscope, rather than continuing to screen deconvolution sets unsuccessfully. As the algorithm that measures mitochondrial length:width reads mitochondria (Tomm20 signal) based on pixel intensity, a better resolution should provide a more accurate 'depiction' of the mitochondrial network, which would be reflected in aspect ratio scores. The Opera confocal microscope improves image quality, and therefore image analysis, because it captures images of greater resolution (pixels per field) than the Cellomics microscope. Even more advantageous is the ability of a confocal microscope to focus on a specific plane, which reduces the background of images and improves the signal to noise when detecting mitochondria[158].

4.3 Identification of MTX2 as a Novel Regulator of Mitochondrial Dynamics

Quantitative analysis of the mitochondrial morphology genome screen is extensive and ongoing as of May, 2014. In the meantime, I developed a shortlist of mitochondrial genes using the Broad Institute's Mitocarta database, and

qualitatively evaluated the images for dramatic changes in mitochondrial morphology. From the screen images I identified siRNA targeting MTX2 as eliciting fragmentation of the mitochondrial network. Deconvolution of pooled MTX2 siRNAs revealed that all 4 siRNA duplexes were able to knockdown MTX2 protein levels, as well as produce fragmentation, indicating that in all likelihood the phenotype was not a result of OTEs[144]. Furthermore, as 4/4 siRNAs exhibited functional correlation between knockdown and phenotype, we were confident that MTX2 was a prime candidate regulator of mitochondrial dynamics. Reintroduction of an siRNA-resistant MTX2 construct is able to partially restore mitochondrial morphology, verifying MTX2's role in maintaining basal mitochondrial morphology. By Western blot, MTX2 levels are not completely restored to control level with MTX2 reintroduction (Figure 10b), which is a likely explanation as to why morphology is also not completely restored to control levels.

4.3.1 MTX2 Regulation

Lentiviral expression of MTX2-V5 results in accumulation of the V5-tagged species at the expense of endogenous MTX2 levels, which are decreased. This observation suggests that MTX2 levels are under strict control by the cell, implying an important biological role for MTX2. Previously, heterogeneous expression of cDNA constructs was a major barrier when trying to rescue candidates. In the case of MTX2, heterogeneous expression was not an issue, as MTX2 levels appear to be unable to accumulate beyond a certain level, resulting

in relatively homogeneous MTX2 expression. Interestingly, endogenous MTX2 levels did not accumulate even after 24h of MG132 treatment, suggesting that the MTX2 protein is normally stable for more than 24h. As MTX2 levels are ablated following 72h of siRNA treatment, MTX2 must be turned over at some point between 24h and 72h. Inhibition of protein translation with cyclohexamide will answer this question. Similarly, MG132 treatment leads to an accumulation of MTX2 species only when MTX2 is overexpressed, raising the possibility that proteasomal regulation of MTX2 is an artifact of overexpression. Experiments measuring MTX2 transcription and translation are required to definitively explain how MTX2 levels are regulated.

4.4 MTX2 Characterization

Having now identified MTX2 as a novel regulator of mitochondrial dynamics, the goal is to elucidate how MTX2 functions to mediate mitochondrial morphology. The MTX2 gene sits on chromosome 2q, and transcribes a 263aa protein of little known function. Armstrong et al. identified MTX2 through a yeast two-hybrid screen using Metaxin 1 (MTX1) as bait[159]. MTX2 lacks a mitochondrial C-terminal membrane anchor domain contained in MTX1, but is proposed to be localized to the OMM through an interaction with MTX1[159]. MTX1 is reported to be an integral membrane component of the mitochondrial preprotein import machinery[160] that is required for embryonic development in mice[161], as well as tumor necrosis factor (TNF)-induced cell death in a murine fibrosarcoma cell line [162]. MTX1 images from the genome screen display fairly

normal mitochondrial morphology as assessed qualitatively (Supp. Fig. 4), suggesting that MTX2 has an independent effect on mitochondrial morphology.

MTX2, along with MTX1, has been implicated in VDAC biogenesis, and loss of MTX2 resulted in deficient protein import into mitochondria[163]. A possible explanation for mitochondrial fragmentation following MTX knockdown, could be loss of membrane potential as a result of deficient protein import, however I demonstrate that loss of MTX2 has no effect on MMP (Supp. Fig. 3). Moreover, MTX2 has been shown to complex with sorting and assembly machinery component 50 (SAM50), coiled-coil-helix-coiled-coil-helix domain 3 (CHCHD3), and mitofilin[164], all of which are known regulators of mitochondrial cristae structure[165-168]. Regulator of IMM fusion, OPA1, is also a critical regulator of cristae structure[37]. These observations may be useful in explaining the loss of OPA1 long isoforms observed following MTX2 knockdown (Figure 11b). As OPA1, mitofilin, and CHCHD3 are IMM proteins, SAM50 is an integral OMM protein, and MTX2 is presumed to be a cytosolic peripherally-associated OMM protein, the precise mechanism of interaction between these proteins as well as how MTX2 affects OPA1 isoform balance requires further clarification.

Very recently, a study by Cartron et al. showed a mechanistic role for MTX2 in apoptosis, through its interaction with the pro-apoptotic protein, BAK[169]. They propose that BAK is normally sequestered on the OMM with VDAC2 and MTX2, but in response to tBid, switches to an association with MTX1, promoting apoptosis. Blocking MTX1 activity with an antibody or siRNA

reduces apoptosis as measured by DEVDase activity and cytochrome C release, whereas inhibiting VDAC2 sensitizes cells to apoptosis by the same metrics[169]. No data demonstrating MTX2's effect on apoptosis was shown, however given its proposed role in a complex with VDAC2, one would predict that loss of MTX2 would also sensitize cells to cytochrome C release. Contrary to the study by Cartron et al, I have experimentally demonstrated that knockdown of MTX2 blocks tBid-induced cytochrome C release (Figure 11c). Further studies are required in order to elucidate the precise role of MTX2 in apoptosis, as well as whether its roles in apoptosis, protein import, and mitochondrial morphology are distinct or have an underlying connection.

4.5 Concluding Remarks

I began my Master's thesis project with the hypothesis that high-throughput siRNA genome screening could identify novel regulators of mitochondrial dynamics. Following a year of unsuccessful attempts to validate candidates, I repeated the genome screen, and was able to identify and confirm MTX2 as a regulator of mitochondrial morphology. While repeating the genome screen did eventually yield a hit, admittedly, MTX2 was found not through unbiased quantitative analysis of the screen data, but through an informed and subjective qualitative analysis of certain genes. Nonetheless, I am confident that once the screen data is properly analyzed and quantified, other genes that affect mitochondrial dynamics will be identified.

Mitochondrial dynamics play an integral role in numerous biological processes required to maintain cellular and organismal health. Illustrating the importance of mitochondrial dynamics, diseases including: cancer, heart disease, neurodegeneration, and diabetes, are all underscored by dysfunction of mediators of mitochondrial morphology. The identification of MTX2 as a novel regulator of mitochondrial morphology provides a new angle from which to study mitochondrial dynamics. Moreover, the functional characterization of MTX2 may lead to the elucidation of novel therapeutic avenues.

Chapter 5. References

1. Benda, C. *Arch. Anat. Physiol.* **73**, 393–398(1898)
2. Lane, N. and W. Martin, *The energetics of genome complexity.* Nature, 2010. **467**(7318): p. 929-34.
3. Friedman, J.R. and J. Nunnari, *Mitochondrial form and function.* Nature, 2014. **505**(7483): p. 335-43.
4. Nunnari, J. and A. Suomalainen, *Mitochondria: in sickness and in health.* Cell, 2012. **148**(6): p. 1145-59.
5. Cogliati, S., et al., *Mitochondrial cristae shape determines respiratory chain supercomplexes assembly and respiratory efficiency.* Cell, 2013. **155**(1): p. 160-71.
6. van der Laan, M., et al., *Role of MINOS in mitochondrial membrane architecture and biogenesis.* Trends Cell Biol, 2012. **22**(4): p. 185-92.
7. Reichert, A.S. and W. Neupert, *Contact sites between the outer and inner membrane of mitochondria-role in protein transport.* Biochim Biophys Acta, 2002. **1592**(1): p. 41-9.
8. Gilkerson, R., et al., *The mitochondrial nucleoid: integrating mitochondrial DNA into cellular homeostasis.* Cold Spring Harb Perspect Biol, 2013. **5**(5): p. a011080.
9. Zick, M., R. Rabl, and A.S. Reichert, *Cristae formation-linking ultrastructure and function of mitochondria.* Biochim Biophys Acta, 2009. **1793**(1): p. 5-19.
10. Acin-Perez, R. and J.A. Enriquez, *The function of the respiratory supercomplexes: the plasticity model.* Biochim Biophys Acta, 2014. **1837**(4): p. 444-50.
11. Strauss, M., et al., *Dimer ribbons of ATP synthase shape the inner mitochondrial membrane.* EMBO J, 2008. **27**(7): p. 1154-60.
12. De Stefani, D., et al., *A forty-kilodalton protein of the inner membrane is the mitochondrial calcium uniporter.* Nature, 2011. **476**(7360): p. 336-40.
13. Lewis, M.R. and W.H. Lewis, *Mitochondria in Tissue Culture.* Science, 1914. **39**(1000): p. 330-3.
14. Bereiter-Hahn, J. and M. Voth, *Dynamics of mitochondria in living cells: shape changes, dislocations, fusion, and fission of mitochondria.* Microsc Res Tech, 1994. **27**(3): p. 198-219.
15. Dhingra, R. and L.A. Kirshenbaum, *Regulation of mitochondrial dynamics and cell fate.* Circ J, 2014. **78**(4): p. 803-10.
16. Westermann, B., *Mitochondrial fusion and fission in cell life and death.* Nat Rev Mol Cell Biol, 2010. **11**(12): p. 872-84.
17. Hoppins, S., *The regulation of mitochondrial dynamics.* Curr Opin Cell Biol, 2014. **29C**: p. 46-52.
18. Santel, A. and M.T. Fuller, *Control of mitochondrial morphology by a human mitofusin.* J Cell Sci, 2001. **114**(Pt 5): p. 867-74.
19. Meeusen, S., et al., *Mitochondrial inner-membrane fusion and crista maintenance requires the dynamin-related GTPase Mgm1.* Cell, 2006. **127**(2): p. 383-95.

20. Koshiba, T., et al., *Structural basis of mitochondrial tethering by mitofusin complexes.* Science, 2004. **305**(5685): p. 858-62.
21. Jensen, R.E. and H. Sesaki, *Ahead of the curve: mitochondrial fusion and phospholipase D.* Nat Cell Biol, 2006. **8**(11): p. 1215-7.
22. Choi, S.Y., et al., *A common lipid links Mfn-mediated mitochondrial fusion and SNARE-regulated exocytosis.* Nat Cell Biol, 2006. **8**(11): p. 1255-62.
23. Huang, H. and M.A. Frohman, *Lipid signaling on the mitochondrial surface.* Biochim Biophys Acta, 2009. **1791**(9): p. 839-44.
24. Tanaka, A., et al., *Proteasome and p97 mediate mitophagy and degradation of mitofusins induced by Parkin.* J Cell Biol, 2010. **191**(7): p. 1367-80.
25. Detmer, S.A. and D.C. Chan, *Complementation between mouse Mfn1 and Mfn2 protects mitochondrial fusion defects caused by CMT2A disease mutations.* J Cell Biol, 2007. **176**(4): p. 405-14.
26. Cipolat, S., et al., *OPA1 requires mitofusin 1 to promote mitochondrial fusion.* Proc Natl Acad Sci U S A, 2004. **101**(45): p. 15927-32.
27. Delettre, C., et al., *Mutation spectrum and splicing variants in the OPA1 gene.* Hum Genet, 2001. **109**(6): p. 584-91.
28. Ishihara, N., et al., *Regulation of mitochondrial morphology through proteolytic cleavage of OPA1.* EMBO J, 2006. **25**(13): p. 2966-77.
29. Griparic, L., T. Kanazawa, and A.M. van der Bliek, *Regulation of the mitochondrial dynamin-like protein Opa1 by proteolytic cleavage.* J Cell Biol, 2007. **178**(5): p. 757-64.
30. Song, Z., et al., *OPA1 processing controls mitochondrial fusion and is regulated by mRNA splicing, membrane potential, and Yme1L.* J Cell Biol, 2007. **178**(5): p. 749-55.
31. Ehses, S., et al., *Regulation of OPA1 processing and mitochondrial fusion by m-AAA protease isoenzymes and OMA1.* J Cell Biol, 2009. **187**(7): p. 1023-36.
32. Head, B., et al., *Inducible proteolytic inactivation of OPA1 mediated by the OMA1 protease in mammalian cells.* J Cell Biol, 2009. **187**(7): p. 959-66.
33. Anand, R., et al., *The i-AAA protease YME1L and OMA1 cleave OPA1 to balance mitochondrial fusion and fission.* J Cell Biol, 2014. **204**(6): p. 919-29.
34. DeVay, R.M., et al., *Coassembly of Mgm1 isoforms requires cardiolipin and mediates mitochondrial inner membrane fusion.* J Cell Biol, 2009. **186**(6): p. 793-803.
35. An, H.J., et al., *Higd-1a interacts with Opa1 and is required for the morphological and functional integrity of mitochondria.* Proc Natl Acad Sci U S A, 2013. **110**(32): p. 13014-9.
36. Arnoult, D., et al., *Release of OPA1 during apoptosis participates in the rapid and complete release of cytochrome c and subsequent mitochondrial fragmentation.* J Biol Chem, 2005. **280**(42): p. 35742-50.
37. Olichon, A., et al., *Loss of OPA1 perturbates the mitochondrial inner membrane structure and integrity, leading to cytochrome c release and apoptosis.* J Biol Chem, 2003. **278**(10): p. 7743-6.
38. Frezza, C., et al., *OPA1 controls apoptotic cristae remodeling independently from mitochondrial fusion.* Cell, 2006. **126**(1): p. 177-89.

39. Sheridan, C., et al., *Bax- or Bak-induced mitochondrial fission can be uncoupled from cytochrome C release.* Mol Cell, 2008. **31**(4): p. 570-85.
40. Breckenridge, D.G., et al., *Caenorhabditis elegans drp-1 and fis-2 regulate distinct cell-death execution pathways downstream of ced-3 and independent of ced-9.* Mol Cell, 2008. **31**(4): p. 586-97.
41. Norton, M., et al., *ROMO1 is an essential redox-dependent regulator of mitochondrial dynamics.* Sci Signal, 2014. **7**(310): p. ra10.
42. Semenzato, M. and L. Scorrano, *O ROM(e)O1, ROM(e)O1, wherefore art thou ROM(e)O1?* Sci Signal, 2014. **7**(310): p. pe2.
43. Mears, J.A., et al., *Conformational changes in Dnm1 support a contractile mechanism for mitochondrial fission.* Nat Struct Mol Biol, 2011. **18**(1): p. 20-6.
44. Smirnova, E., et al., *Dynamin-related protein Drp1 is required for mitochondrial division in mammalian cells.* Mol Biol Cell, 2001. **12**(8): p. 2245-56.
45. Smirnova, E., et al., *A human dynamin-related protein controls the distribution of mitochondria.* J Cell Biol, 1998. **143**(2): p. 351-8.
46. Loson, O.C., et al., *Fis1, Mff, MiD49, and MiD51 mediate Drp1 recruitment in mitochondrial fission.* Mol Biol Cell, 2013. **24**(5): p. 659-67.
47. Friedman, J.R., et al., *ER tubules mark sites of mitochondrial division.* Science, 2011. **334**(6054): p. 358-62.
48. Chang, C.R. and C. Blackstone, *Cyclic AMP-dependent protein kinase phosphorylation of Drp1 regulates its GTPase activity and mitochondrial morphology.* J Biol Chem, 2007. **282**(30): p. 21583-7.
49. Gomes, L.C., G. Di Benedetto, and L. Scorrano, *During autophagy mitochondria elongate, are spared from degradation and sustain cell viability.* Nat Cell Biol, 2011. **13**(5): p. 589-98.
50. Cereghetti, G.M., et al., *Dephosphorylation by calcineurin regulates translocation of Drp1 to mitochondria.* Proc Natl Acad Sci U S A, 2008. **105**(41): p. 15803-8.
51. Taguchi, N., et al., *Mitotic phosphorylation of dynamin-related GTPase Drp1 participates in mitochondrial fission.* J Biol Chem, 2007. **282**(15): p. 11521-9.
52. Wang, H., et al., *Parkin ubiquitinates Drp1 for proteasome-dependent degradation: implication of dysregulated mitochondrial dynamics in Parkinson disease.* J Biol Chem, 2011. **286**(13): p. 11649-58.
53. Nakamura, N., et al., *MARCH-V is a novel mitofusin 2- and Drp1-binding protein able to change mitochondrial morphology.* EMBO Rep, 2006. **7**(10): p. 1019-22.
54. Fang, L., et al., *MARCH5 inactivation supports mitochondrial function during neurodegenerative stress.* Front Cell Neurosci, 2013. **7**: p. 176.
55. Karbowski, M., A. Neutzner, and R.J. Youle, *The mitochondrial E3 ubiquitin ligase MARCH5 is required for Drp1 dependent mitochondrial division.* J Cell Biol, 2007. **178**(1): p. 71-84.
56. Park, Y.Y., et al., *Loss of MARCH5 mitochondrial E3 ubiquitin ligase induces cellular senescence through dynamin-related protein 1 and mitofusin 1.* J Cell Sci, 2010. **123**(Pt 4): p. 619-26.

57. Karbowski, M., et al., *Role of Bax and Bak in mitochondrial morphogenesis.* Nature, 2006. **443**(7112): p. 658-62.
58. Wasiak, S., R. Zunino, and H.M. McBride, *Bax/Bak promote sumoylation of DRP1 and its stable association with mitochondria during apoptotic cell death.* J Cell Biol, 2007. **177**(3): p. 439-50.
59. Harder, Z., R. Zunino, and H. McBride, *Sumo1 conjugates mitochondrial substrates and participates in mitochondrial fission.* Curr Biol, 2004. **14**(4): p. 340-5.
60. Figueroa-Romero, C., et al., *SUMOylation of the mitochondrial fission protein Drp1 occurs at multiple nonconsensus sites within the B domain and is linked to its activity cycle.* FASEB J, 2009. **23**(11): p. 3917-27.
61. Braschi, E., R. Zunino, and H.M. McBride, *MAPL is a new mitochondrial SUMO E3 ligase that regulates mitochondrial fission.* EMBO Rep, 2009. **10**(7): p. 748-54.
62. Zunino, R., et al., *Translocation of SenP5 from the nucleoli to the mitochondria modulates DRP1-dependent fission during mitosis.* J Biol Chem, 2009. **284**(26): p. 17783-95.
63. Zunino, R., et al., *The SUMO protease SENP5 is required to maintain mitochondrial morphology and function.* J Cell Sci, 2007. **120**(Pt 7): p. 1178-88.
64. Gandre-Babbe, S. and A.M. van der Bliek, *The novel tail-anchored membrane protein Mff controls mitochondrial and peroxisomal fission in mammalian cells.* Mol Biol Cell, 2008. **19**(6): p. 2402-12.
65. Otera, H., et al., *Mff is an essential factor for mitochondrial recruitment of Drp1 during mitochondrial fission in mammalian cells.* J Cell Biol, 2010. **191**(6): p. 1141-58.
66. Mozdy, A.D., J.M. McCaffery, and J.M. Shaw, *Dnm1p GTPase-mediated mitochondrial fission is a multi-step process requiring the novel integral membrane component Fis1p.* J Cell Biol, 2000. **151**(2): p. 367-80.
67. Tieu, Q. and J. Nunnari, *Mdv1p is a WD repeat protein that interacts with the dynamin-related GTPase, Dnm1p, to trigger mitochondrial division.* J Cell Biol, 2000. **151**(2): p. 353-66.
68. Yoon, Y., et al., *The mitochondrial protein hFis1 regulates mitochondrial fission in mammalian cells through an interaction with the dynamin-like protein DLP1.* Mol Cell Biol, 2003. **23**(15): p. 5409-20.
69. Palmer, C.S., et al., *MiD49 and MiD51, new components of the mitochondrial fission machinery.* EMBO Rep, 2011. **12**(6): p. 565-73.
70. Zhao, J., et al., *Human MIEF1 recruits Drp1 to mitochondrial outer membranes and promotes mitochondrial fusion rather than fission.* EMBO J, 2011. **30**(14): p. 2762-78.
71. Palmer, C.S., et al., *Adaptor proteins MiD49 and MiD51 can act independently of Mff and Fis1 in Drp1 recruitment and are specific for mitochondrial fission.* J Biol Chem, 2013. **288**(38): p. 27584-93.
72. Gillies, L.A. and T. Kuwana, *Apoptosis regulation at the mitochondrial outer membrane.* J Cell Biochem, 2014. **115**(4): p. 632-40.

73. Fulda, S. and K.M. Debatin, *Extrinsic versus intrinsic apoptosis pathways in anticancer chemotherapy.* Oncogene, 2006. **25**(34): p. 4798-811.
74. Lin, M.T. and M.F. Beal, *Mitochondrial dysfunction and oxidative stress in neurodegenerative diseases.* Nature, 2006. **443**(7113): p. 787-95.
75. Degterev, A., M. Boyce, and J. Yuan, *A decade of caspases.* Oncogene, 2003. **22**(53): p. 8543-67.
76. Suen, D.F., K.L. Norris, and R.J. Youle, *Mitochondrial dynamics and apoptosis.* Genes Dev, 2008. **22**(12): p. 1577-90.
77. Liu, X., et al., *Induction of apoptotic program in cell-free extracts: requirement for dATP and cytochrome c.* Cell, 1996. **86**(1): p. 147-57.
78. Martinou, J.C. and R.J. Youle, *Mitochondria in apoptosis: Bcl-2 family members and mitochondrial dynamics.* Dev Cell, 2011. **21**(1): p. 92-101.
79. De Vos, K., et al., *The 55-kDa tumor necrosis factor receptor induces clustering of mitochondria through its membrane-proximal region.* J Biol Chem, 1998. **273**(16): p. 9673-80.
80. Saraste, A. and K. Pulkki, *Morphologic and biochemical hallmarks of apoptosis.* Cardiovasc Res, 2000. **45**(3): p. 528-37.
81. Frank, S., et al., *The role of dynamin-related protein 1, a mediator of mitochondrial fission, in apoptosis.* Dev Cell, 2001. **1**(4): p. 515-25.
82. Karbowski, M., et al., *Spatial and temporal association of Bax with mitochondrial fission sites, Drp1, and Mfn2 during apoptosis.* J Cell Biol, 2002. **159**(6): p. 931-8.
83. Lee, Y.J., et al., *Roles of the mammalian mitochondrial fission and fusion mediators Fis1, Drp1, and Opa1 in apoptosis.* Mol Biol Cell, 2004. **15**(11): p. 5001-11.
84. Karbowski, M., et al., *Quantitation of mitochondrial dynamics by photolabeling of individual organelles shows that mitochondrial fusion is blocked during the Bax activation phase of apoptosis.* J Cell Biol, 2004. **164**(4): p. 493-9.
85. Tondera, D., et al., *SLP-2 is required for stress-induced mitochondrial hyperfusion.* EMBO J, 2009. **28**(11): p. 1589-600.
86. Olichon, A., et al., *Mitochondrial dynamics and disease, OPA1.* Biochim Biophys Acta, 2006. **1763**(5-6): p. 500-9.
87. Chen, H., et al., *Mitofusins Mfn1 and Mfn2 coordinately regulate mitochondrial fusion and are essential for embryonic development.* J Cell Biol, 2003. **160**(2): p. 189-200.
88. Davies, V.J., et al., *Opa1 deficiency in a mouse model of autosomal dominant optic atrophy impairs mitochondrial morphology, optic nerve structure and visual function.* Hum Mol Genet, 2007. **16**(11): p. 1307-18.
89. Ishihara, N., et al., *Mitochondrial fission factor Drp1 is essential for embryonic development and synapse formation in mice.* Nat Cell Biol, 2009. **11**(8): p. 958-66.
90. Waterham, H.R., et al., *A lethal defect of mitochondrial and peroxisomal fission.* N Engl J Med, 2007. **356**(17): p. 1736-41.
91. Hong, Z., et al., *Role of dynamin-related protein 1 (Drp1)-mediated mitochondrial fission in oxygen sensing and constriction of the ductus arteriosus.* Circ Res, 2013. **112**(5): p. 802-15.

92. Ly, C.V. and P. Verstreken, *Mitochondria at the synapse.* Neuroscientist, 2006. **12**(4): p. 291-9.
93. Mitra, K., et al., *A hyperfused mitochondrial state achieved at G1-S regulates cyclin E buildup and entry into S phase.* Proc Natl Acad Sci U S A, 2009. **106**(29): p. 11960-5.
94. Chen, H., J.M. McCaffery, and D.C. Chan, *Mitochondrial fusion protects against neurodegeneration in the cerebellum.* Cell, 2007. **130**(3): p. 548-62.
95. Gilkerson, R.W., et al., *Mitochondrial nucleoids maintain genetic autonomy but allow for functional complementation.* J Cell Biol, 2008. **181**(7): p. 1117-28.
96. Wikstrom, J.D., G. Twig, and O.S. Shirihai, *What can mitochondrial heterogeneity tell us about mitochondrial dynamics and autophagy?* Int J Biochem Cell Biol, 2009. **41**(10): p. 1914-27.
97. Kmiec, B., M. Woloszynska, and H. Janska, *Heteroplasmy as a common state of mitochondrial genetic information in plants and animals.* Curr Genet, 2006. **50**(3): p. 149-59.
98. Chen, H., A. Chomyn, and D.C. Chan, *Disruption of fusion results in mitochondrial heterogeneity and dysfunction.* J Biol Chem, 2005. **280**(28): p. 26185-92.
99. Twig, G., et al., *Fission and selective fusion govern mitochondrial segregation and elimination by autophagy.* EMBO J, 2008. **27**(2): p. 433-46.
100. Greene, A.W., et al., *Mitochondrial processing peptidase regulates PINK1 processing, import and Parkin recruitment.* EMBO Rep, 2012. **13**(4): p. 378-85.
101. Jin, S.M., et al., *Mitochondrial membrane potential regulates PINK1 import and proteolytic destabilization by PARL.* J Cell Biol, 2010. **191**(5): p. 933-42.
102. Narendra, D.P., et al., *PINK1 is selectively stabilized on impaired mitochondria to activate Parkin.* PLoS Biol, 2010. **8**(1): p. e1000298.
103. Kawajiri, S., et al., *PINK1 is recruited to mitochondria with parkin and associates with LC3 in mitophagy.* FEBS Lett, 2010. **584**(6): p. 1073-9.
104. Matsuda, N., et al., *PINK1 stabilized by mitochondrial depolarization recruits Parkin to damaged mitochondria and activates latent Parkin for mitophagy.* J Cell Biol, 2010. **189**(2): p. 211-21.
105. Vives-Bauza, C., et al., *PINK1/Parkin direct mitochondria to autophagy.* Autophagy, 2010. **6**(2): p. 315-6.
106. Vives-Bauza, C., et al., *PINK1-dependent recruitment of Parkin to mitochondria in mitophagy.* Proc Natl Acad Sci U S A, 2010. **107**(1): p. 378-83.
107. Narendra, D., et al., *Parkin is recruited selectively to impaired mitochondria and promotes their autophagy.* J Cell Biol, 2008. **183**(5): p. 795-803.
108. Chen, Y. and G.W. Dorn, 2nd, *PINK1-phosphorylated mitofusin 2 is a Parkin receptor for culling damaged mitochondria.* Science, 2013. **340**(6131): p. 471-5.
109. Hanahan, D. and R.A. Weinberg, *Hallmarks of cancer: the next generation.* Cell, 2011. **144**(5): p. 646-74.
110. Archer, S.L., *Mitochondrial dynamics--mitochondrial fission and fusion in human diseases.* N Engl J Med, 2013. **369**(23): p. 2236-51.

111. Rehman, J., et al., *Inhibition of mitochondrial fission prevents cell cycle progression in lung cancer.* FASEB J, 2012. **26**(5): p. 2175-86.
112. Chiang, Y.Y., et al., *Nuclear expression of dynamin-related protein 1 in lung adenocarcinomas.* Mod Pathol, 2009. **22**(9): p. 1139-50.
113. Hagenbuchner, J., et al., *BIRC5/Survivin enhances aerobic glycolysis and drug resistance by altered regulation of the mitochondrial fusion/fission machinery.* Oncogene, 2012.
114. Scatena, R., *Mitochondria and cancer: a growing role in apoptosis, cancer cell metabolism and dedifferentiation.* Adv Exp Med Biol, 2012. **942**: p. 287-308.
115. Ryan, J.J., et al., *PGC1alpha-mediated mitofusin-2 deficiency in female rats and humans with pulmonary arterial hypertension.* Am J Respir Crit Care Med, 2013. **187**(8): p. 865-78.
116. Marsboom, G., et al., *Dynamin-related protein 1-mediated mitochondrial mitotic fission permits hyperproliferation of vascular smooth muscle cells and offers a novel therapeutic target in pulmonary hypertension.* Circ Res, 2012. **110**(11): p. 1484-97.
117. Chen, L., et al., *Mitochondrial OPA1, apoptosis, and heart failure.* Cardiovasc Res, 2009. **84**(1): p. 91-9.
118. Sharp, W.W., et al., *Dynamin-related protein 1 (Drp1)-mediated diastolic dysfunction in myocardial ischemia-reperfusion injury: therapeutic benefits of Drp1 inhibition to reduce mitochondrial fission.* FASEB J, 2014. **28**(1): p. 316-26.
119. Chen, H. and D.C. Chan, *Mitochondrial dynamics--fusion, fission, movement, and mitophagy--in neurodegenerative diseases.* Hum Mol Genet, 2009. **18**(R2): p. R169-76.
120. Subramaniam, S.R. and M.F. Chesselet, *Mitochondrial dysfunction and oxidative stress in Parkinson's disease.* Prog Neurobiol, 2013. **106-107**: p. 17-32.
121. Schapira, A.H., *Mitochondria in the aetiology and pathogenesis of Parkinson's disease.* Lancet Neurol, 2008. **7**(1): p. 97-109.
122. Wang, H., et al., *Effects of overexpression of huntingtin proteins on mitochondrial integrity.* Hum Mol Genet, 2009. **18**(4): p. 737-52.
123. Song, W., et al., *Mutant huntingtin binds the mitochondrial fission GTPase dynamin-related protein-1 and increases its enzymatic activity.* Nat Med, 2011. **17**(3): p. 377-82.
124. Wang, X., et al., *Amyloid-beta overproduction causes abnormal mitochondrial dynamics via differential modulation of mitochondrial fission/fusion proteins.* Proc Natl Acad Sci U S A, 2008. **105**(49): p. 19318-23.
125. Wang, X., et al., *Impaired balance of mitochondrial fission and fusion in Alzheimer's disease.* J Neurosci, 2009. **29**(28): p. 9090-103.
126. Grohm, J., et al., *Inhibition of Drp1 provides neuroprotection in vitro and in vivo.* Cell Death Differ, 2012. **19**(9): p. 1446-58.
127. Zuchner, S., et al., *Mutations in the mitochondrial GTPase mitofusin 2 cause Charcot-Marie-Tooth neuropathy type 2A.* Nat Genet, 2004. **36**(5): p. 449-51.
128. Del Bo, R., et al., *Mutated mitofusin 2 presents with intrafamilial variability and brain mitochondrial dysfunction.* Neurology, 2008. **71**(24): p. 1959-66.

129. Zuchner, S. and J.M. Vance, *Mechanisms of disease: a molecular genetic update on hereditary axonal neuropathies.* Nat Clin Pract Neurol, 2006. **2**(1): p. 45-53.
130. Zorzano, A., M. Liesa, and M. Palacin, *Role of mitochondrial dynamics proteins in the pathophysiology of obesity and type 2 diabetes.* Int J Biochem Cell Biol, 2009. **41**(10): p. 1846-54.
131. Sebastian, D., et al., *Mitofusin 2 (Mfn2) links mitochondrial and endoplasmic reticulum function with insulin signaling and is essential for normal glucose homeostasis.* Proc Natl Acad Sci U S A, 2012. **109**(14): p. 5523-8.
132. Zhang, Z., et al., *The dynamin-related GTPase Opa1 is required for glucose-stimulated ATP production in pancreatic beta cells.* Mol Biol Cell, 2011. **22**(13): p. 2235-45.
133. Fire, A., et al., *Potent and specific genetic interference by double-stranded RNA in Caenorhabditis elegans.* Nature, 1998. **391**(6669): p. 806-11.
134. Hannon, G.J., *RNA interference.* Nature, 2002. **418**(6894): p. 244-51.
135. Waterhouse, P.M., M.B. Wang, and T. Lough, *Gene silencing as an adaptive defence against viruses.* Nature, 2001. **411**(6839): p. 834-42.
136. Meister, G. and T. Tuschl, *Mechanisms of gene silencing by double-stranded RNA.* Nature, 2004. **431**(7006): p. 343-9.
137. Friedman, R.C., et al., *Most mammalian mRNAs are conserved targets of microRNAs.* Genome Res, 2009. **19**(1): p. 92-105.
138. Elbashir, S.M., et al., *Duplexes of 21-nucleotide RNAs mediate RNA interference in cultured mammalian cells.* Nature, 2001. **411**(6836): p. 494-8.
139. Matranga, C., et al., *Passenger-strand cleavage facilitates assembly of siRNA into Ago2-containing RNAi enzyme complexes.* Cell, 2005. **123**(4): p. 607-20.
140. Czech, B. and G.J. Hannon, *Small RNA sorting: matchmaking for Argonautes.* Nat Rev Genet, 2011. **12**(1): p. 19-31.
141. Rand, T.A., et al., *Argonaute2 cleaves the anti-guide strand of siRNA during RISC activation.* Cell, 2005. **123**(4): p. 621-9.
142. Meister, G., et al., *Human Argonaute2 mediates RNA cleavage targeted by miRNAs and siRNAs.* Mol Cell, 2004. **15**(2): p. 185-97.
143. Ghildiyal, M. and P.D. Zamore, *Small silencing RNAs: an expanding universe.* Nat Rev Genet, 2009. **10**(2): p. 94-108.
144. *Whither RNAi?* Nat Cell Biol, 2003. **5**(6): p. 489-90.
145. Malo, N., et al., *Statistical practice in high-throughput screening data analysis.* Nat Biotechnol, 2006. **24**(2): p. 167-75.
146. Sharma, S. and A. Rao, *RNAi screening: tips and techniques.* Nat Immunol, 2009. **10**(8): p. 799-804.
147. Echeverri, C.J. and N. Perrimon, *High-throughput RNAi screening in cultured cells: a user's guide.* Nat Rev Genet, 2006. **7**(5): p. 373-84.
148. Oberdoerffer, S., et al., *Regulation of CD45 alternative splicing by heterogeneous ribonucleoprotein, hnRNPLL.* Science, 2008. **321**(5889): p. 686-91.
149. Chen, Z., et al., *Modeling CTLA4-linked autoimmunity with RNA interference in mice.* Proc Natl Acad Sci U S A, 2006. **103**(44): p. 16400-5.

150. Jackson, A.L. and P.S. Linsley, *Recognizing and avoiding siRNA off-target effects for target identification and therapeutic application.* Nat Rev Drug Discov, 2010. **9**(1): p. 57-67.
151. Sigoillot, F.D. and R.W. King, *Vigilance and validation: Keys to success in RNAi screening.* ACS Chem Biol, 2011. **6**(1): p. 47-60.
152. Echeverri, C.J., et al., *Minimizing the risk of reporting false positives in large-scale RNAi screens.* Nat Methods, 2006. **3**(10): p. 777-9.
153. Khan, A.A., et al., *Transfection of small RNAs globally perturbs gene regulation by endogenous microRNAs.* Nat Biotechnol, 2009. **27**(6): p. 549-55.
154. Birmingham, A., et al., *Statistical methods for analysis of high-throughput RNA interference screens.* Nat Methods, 2009. **6**(8): p. 569-75.
155. Wiles, A.M., et al., *An analysis of normalization methods for Drosophila RNAi genomic screens and development of a robust validation scheme.* J Biomol Screen, 2008. **13**(8): p. 777-84.
156. Chung, N., et al., *Median absolute deviation to improve hit selection for genome-scale RNAi screens.* J Biomol Screen, 2008. **13**(2): p. 149-58.
157. Cullen, B.R., *Enhancing and confirming the specificity of RNAi experiments.* Nat Methods, 2006. **3**(9): p. 677-81.
158. Robinson, J.P., *Principles of confocal microscopy.* Methods Cell Biol, 2001. **63**: p. 89-106.
159. Armstrong, L.C., A.J. Saenz, and P. Bornstein, *Metaxin 1 interacts with metaxin 2, a novel related protein associated with the mammalian mitochondrial outer membrane.* J Cell Biochem, 1999. **74**(1): p. 11-22.
160. Armstrong, L.C., et al., *Metaxin is a component of a preprotein import complex in the outer membrane of the mammalian mitochondrion.* J Biol Chem, 1997. **272**(10): p. 6510-8.
161. Bornstein, P., et al., *Metaxin, a gene contiguous to both thrombospondin 3 and glucocerebrosidase, is required for embryonic development in the mouse: implications for Gaucher disease.* Proc Natl Acad Sci U S A, 1995. **92**(10): p. 4547-51.
162. Wang, X., et al., *Metaxin is required for tumor necrosis factor-induced cell death.* EMBO Rep, 2001. **2**(7): p. 628-33.
163. Kozjak-Pavlovic, V., et al., *Conserved roles of Sam50 and metaxins in VDAC biogenesis.* EMBO Rep, 2007. **8**(6): p. 576-82.
164. Xie, J., et al., *The mitochondrial inner membrane protein mitofilin exists as a complex with SAM50, metaxins 1 and 2, coiled-coil-helix coiled-coil-helix domain-containing protein 3 and 6 and DnaJC11.* FEBS Lett, 2007. **581**(18): p. 3545-9.
165. Darshi, M., et al., *ChChd3, an inner mitochondrial membrane protein, is essential for maintaining crista integrity and mitochondrial function.* J Biol Chem, 2011. **286**(4): p. 2918-32.
166. John, G.B., et al., *The mitochondrial inner membrane protein mitofilin controls cristae morphology.* Mol Biol Cell, 2005. **16**(3): p. 1543-54.
167. Ott, C., et al., *Sam50 functions in mitochondrial intermembrane space bridging and biogenesis of respiratory complexes.* Mol Cell Biol, 2012. **32**(6): p. 1173-88.

168. von der Malsburg, K., et al., *Dual role of mitofilin in mitochondrial membrane organization and protein biogenesis.* Dev Cell, 2011. **21**(4): p. 694-707.
169. Cartron, P.F., et al., *Metaxins 1 and 2, two proteins of the mitochondrial protein sorting and assembly machinery, are essential for Bak activation during TNF alpha triggered apoptosis.* Cell Signal, 2014.

Chapter 6. Appendix

Supplementary Figures

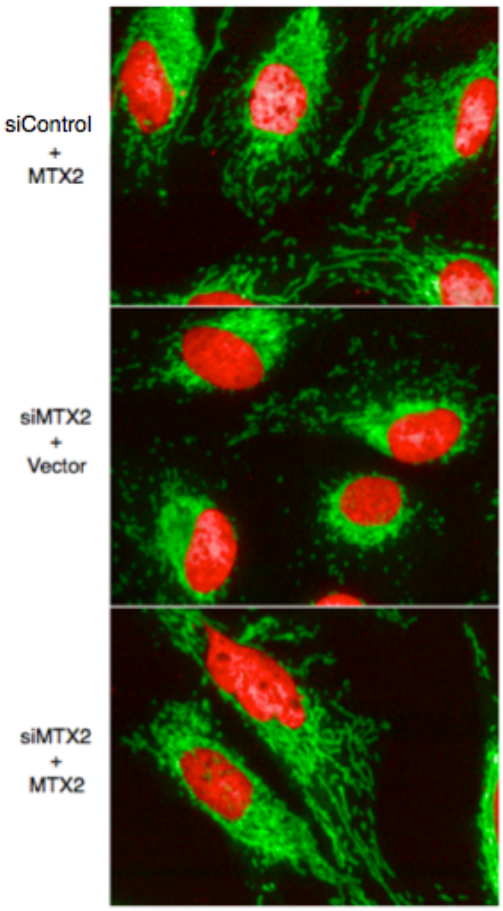

Supplementary Figure 1. Reintroduction of MTX2 Restores Normal Mitochondrial Morphology. HeLa cells transfected with Control or MTX2 siRNA, and infected with lentivirus carrying Vector or an siRNA-resistant MTX2 cDNA were stained with Hoechst (red) and Tomm20 (green), and imaged on the Opera confocal microscope at 40X magnification. Representative fields of images are shown. Images were captured from the same plate as used for rescue quantification in Figure 10.

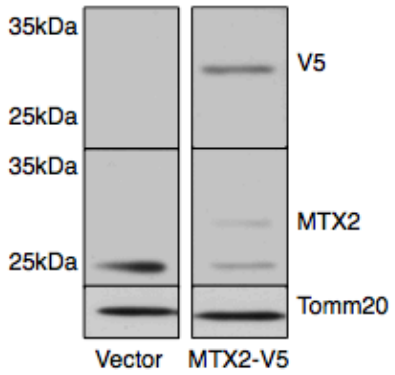

Supplementary Figure 2. Identification of MTX-V5 by Western blot. 293T cells were transfected with the indicated plasmids for 72h, before being harvested. Protein was separated by SDS PAGE. Probing for MTX2 reveals two bands: the lower band corresponds to endogenous MTX2, whereas the upper band corresponds to MTX2-V5. This was confirmed by probing for V5, which exposes a band at exactly the same molecular weight of MTX2-V5, thus confirming that the higher species is MTX2-V5. WB was cropped to show only the relevant lanes.

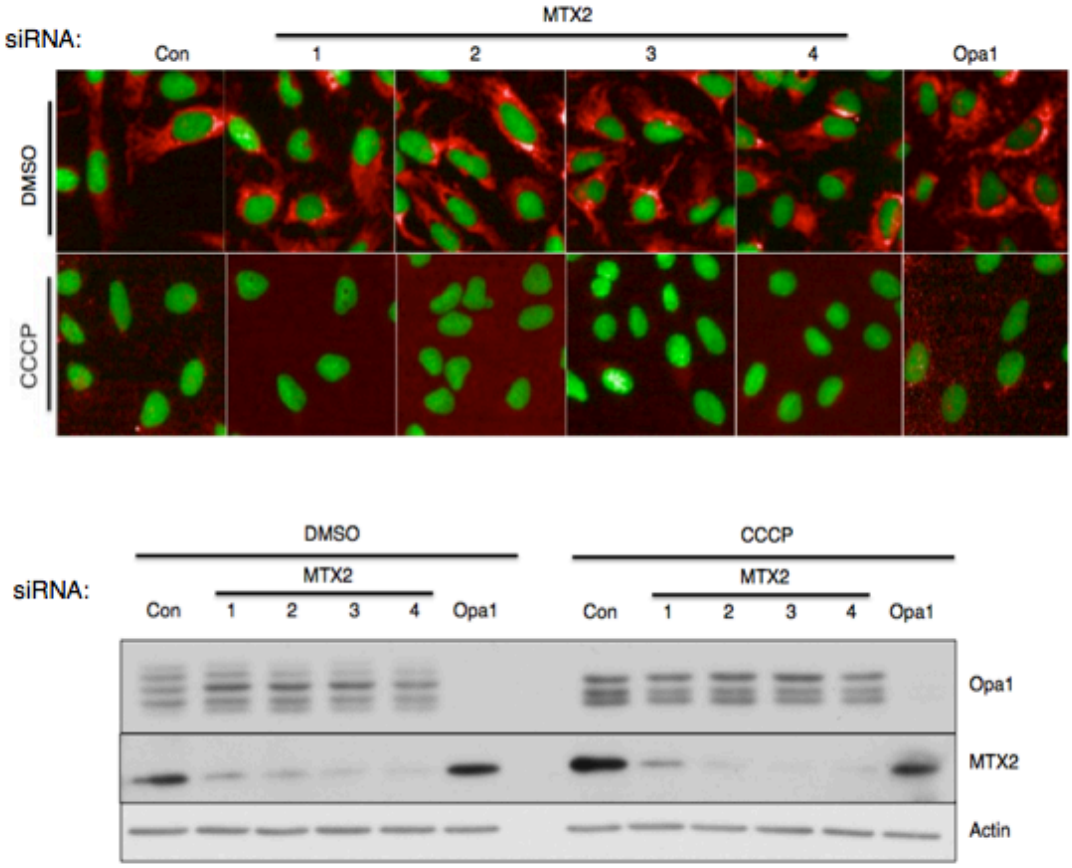

Supplementary Figure 3. Knockdown of MTX2 Does Not Affect Mitochondrial Membrane Potential. 72h following transfection, U2OS cells were loaded with the mitochondria-specific, potentiometric dye, TMRE, and Hoechst for 1h, then treated with DMSO, or the protonophore, CCCP, for 1h, prior to undergoing live cell image analysis (Mitochondria are in red; nuclei are green). Knockdown of MTX2 had no effect on mitochondrial membrane potential. CCCP treatment completely dissipates mitochondrial membrane potential. Effect of CCCP treatment on OPA1 oligomers is shown by parallel WB.

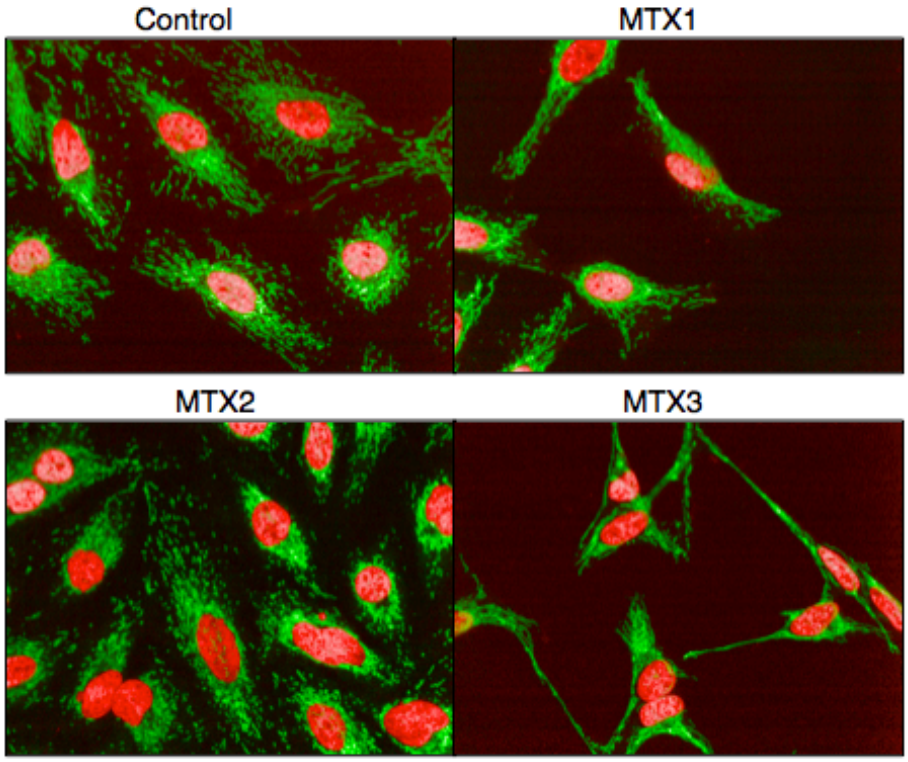

Supplementary Figure 4. Screen Images of Metaxin Homologues. Genome screen images for HeLa cells transfected with siRNA targeting the three human metaxin homologues. Only MTX2 displays fragmentation, whereas MTX1 has no phenotype and MTX3 is slightly elongated. MTX1 and MTX3 siRNAs displayed some toxicity. Images are one field captured by the Opera confocal microscope at 40X magnification. Mitochondria are in green, nuclei are in red.